

Modelling and start-up optimization of a coal-fired power plant

Håkan Runvik



LUND
UNIVERSITY

Department of Automatic Control

MSc Thesis
ISRN LUTFD2/TFRT--5950--SE
ISSN 0280-5316

Department of Automatic Control
Lund University
Box 118
SE-221 00 LUND
Sweden

© 2014 by Håkan Runvik. All rights reserved.
Printed in Sweden by Media-Tryck.
Lund 2014

Abstract

In the German electrical market, where almost no hydro power is present, the demand for regulating power is rising. The main reason for this is the expansion of solar and wind power, which is desirable from an environmental standpoint, but also introduces large and fast variations in production. To keep the necessary balance between production and consumption, the operation of thermal power plants is changing, both in terms of stand still time and load variations. For this reason the start-up procedure of the Vattenfall owned German lignite power plant Jänschwalde is investigated in this thesis.

A model is created that is complex enough to describe the behaviour of the real plant reasonably accurately, while at the same time simple enough so that optimization of it can be performed with the optimization platform JModelica.org. A detailed plant developed in another thesis is used to determine parameter values and validate the behaviour of the optimization model during simulation. The start-up procedure is handled as an optimal control problem, with constraints on stress in order to avoid damage and maximize the life length of components. Results for different optimization cases are finally calculated and compared.

Keywords: JModelica.org, Dynamic optimization, Modelica, Control, Modelling, Thermal power plants

Acknowledgements

My biggest gratitude goes to my supervisor Stéphane Velut at Modelon AB, who have helped me in numerous ways. His guidance regarding dynamic optimization and JModelica.org, as well as the general planning of the project have been outstanding.

I would also like to thank Jonas Funkquist and the rest of the team at Vattenfall AB, who have provided much insights into how thermal power plants and their control systems work.

This work was conducted within the ITEA3 project MODRIO, which has the aim to "extend state-of-the-art modelling and simulation environments based on open standards to increase energy and transportation systems safety, dependability and performance throughout their lifecycle" [*MODRIO*].

Contents

List of Figures	9
List of Tables	11
1. Introduction	12
1.1 Aim of thesis	13
1.2 Structure of thesis	13
2. Background	14
2.1 Power plant	14
2.2 Theory	21
3. Dynamic optimization	25
3.1 Differential algebraic equations	25
3.2 DAE optimization problem	25
3.3 Non-linear programming	27
3.4 Interior point method	27
4. Programs and tools	29
4.1 Modelica and Dymola	29
4.2 Optimica	30
4.3 JModelica.org	30
5. Modelling	33
5.1 Detailed model	33
5.2 Media models	33
5.3 Start-up optimization model	34
5.4 Units	37
5.5 Boundary conditions and model simplifications	37
5.6 Calibration	38
6. Optimization	41
6.1 Building an optimization model	41
6.2 Constraint calculation	43
6.3 Optimization cases	44
6.4 Initialization	44

Contents

6.5	Optimization settings	45
7.	Results	47
7.1	Phase 1	47
7.2	Phase 2	50
8.	Discussion and Conclusions	56
8.1	Modelling	56
8.2	Optimization	57
8.3	Experiences with JModelica.org	58
8.4	Conclusion	59
	Bibliography	60

List of Figures

2.1	Overview of a coal fired power plant. The superheaters and reheaters are denoted SH and RH, respectively, while LPP and HPP are the low pressure and high pressure preheaters. HP-T, IP-T, and L-T are different turbine stages.	14
2.2	T-s (temperature vs entropy) diagram of the Carnot cycle.	15
2.3	T-s diagram of the Rankine cycle with reheat.	16
2.4	Different measured signals during a cold start-up of a block at the Jän-schwalde power plant. Each block has two boilers which are started separately, named 1 and 2 in the legends. On top the coal feeder speed is illustrated, below is the water and steam flow, and the bottom plot shows the steam temperature at different points in the steam cycle. . .	19
2.5	The top plot shows the turbine speed. The electric power output is plotted in the middle, together with setpoints and the load schedule, which is a reference signal for the production of the plant. Different valve positions are displayed in the bottom plot. Maximum load is reached after 18 hours.	20
2.6	Typical header design.	22
2.7	Life time calculation using the Wöhler-curve.	24
2.8	Maximal stress amplitude giving minimum stress constraint.	24
3.1	An element with two collocation points q_1 and q_2	27
4.1	IPOPT output	32
5.1	Overview of the detailed plant model in Dymola.	34
5.2	The optimization plant model.	35
5.3	Gas and steam output temperatures for superheater 1. The input gas mass flow and temperature are ramped in two separate stages.	39

7.1 The calculated optimal trajectories for phase 1, case 1 in blue together with simulation results with the optimal control signals as input in green. Dashed in red and purple are the active constraints and the setpoints, respectively. One can note that the optimization algorithm manages to represent the system model well, as the difference between the curves is small. The pressure and gas mass flow are ramped at maximal speed. For the gas mass flow a large overshoot compared to the final steady state behaviour can be observed, which makes the temperature reach its setpoint faster. 48

7.2 The calculated optimal trajectories for phase 1, case 2 in blue and case 3 in green, together with the active constraints marked with dashed red and the desired levels in dashed purple. The active stress constraint forces a reduced increase in gas mass flow compared to case 1. For case 3 only monotonously increasing gas mass flow is allowed. The most notable result for this case is that the live steam pressure does not remain at its desired value for the second half of the optimization time, while the gas mass flow is significantly higher than in case 2. The optimization algorithm prioritizes the faster increase in SH4 temperature the higher mass flow induces over keeping the live steam pressure setpoint. A small deviation from the temperature setpoint can also be observed. 49

7.3 The calculated optimal trajectories for phase 2, case 1 in blue, together with constraints marked with dashed red, and the desired SH4 temperature in dashed purple. The gas mass flow is ramped without any overshoot. The stress constraint is not active, yet the bypass valve is reopened. 51

7.4 The calculated optimal trajectories for phase 2, case 2 in blue, together with simulation results based on the optimization results with (green) and without (pink, dashed) the bypass reopening in the SH4 temperature and bypass valve plots. Constraints are marked in dashed red and the temperature setpoint in dashed purple. 52

7.5 A comparison of the calculated optimal trajectories for phase 2, case 3 (blue) and 4 (green). Active constraints are marked in dashed red and the SH4 temperature setpoint is marked in dashed purple. The monotonous valve ratio forces more mass flow control actions in case 4, in order to prevent the stress constraint from being violated. 53

7.6 The calculated optimal trajectories for phase 2, case 4 in green and case 5 in blue, together with constraints marked with dashed red and the desired SH4 temperature in dashed purple. The control action is similar for the two cases. 54

7.7	The calculated optimal trajectories for phase 2, case 5 in blue and case 6 in green, together with constraints marked with dashed red and the desired SH4 temperature in dashed purple. In case 6 the further relaxed gas mass flow constraint results in a slightly longer period with stress close to the limit compared to case 5.	55
-----	---	----

List of Tables

2.1	The steam cycle of a thermal power plant. The steps refer to figure 2.3.	17
2.2	Start-ups of the Jämschwalde plant	17
5.1	Heat transfer parameter values.	39
5.2	Full load heat exchanger temperature comparison.	40
6.1	Critical component stress level calculations.	43
6.2	Optimization solver options	45
7.1	The different optimization cases for phase 1. For the cases with reduced stress an SH4 header stress constraint of -30 MPa is used.	47
7.2	Optimization convergence data for phase 1. T_{calc} is the calculation time for the solver IPOPT.	47
7.3	Different cost function weights give different optimization cases. In case 5 and 6 16 elements were used, while 10 elements were used in the rest of the cases.	50
7.4	Optimization convergence data for phase 2. T_{calc} is the calculation time for the solver IPOPT.	50

1

Introduction

The start-up of a thermal power plant is a complicated process with many aspects to consider. By conducting it efficiently environmental as well as financial gains can be achieved. The importance of the start-up schedules of thermal power plants in Germany is increasing as more wind and solar power is being installed in order to reduce the carbon dioxide emissions. To compensate for the variations in production the renewable sources introduce, more regulating power is needed. Hydro power is very suitable for this purpose, but in Germany mainly thermal power is used instead. The operation of thermal power plants is therefore changing in several ways, one of which is an increasing number of start-ups per year.

The start-up of the German lignite power plant Jänschwalde is examined in this thesis. A simplified model of the plant is developed and a start-up scenario is considered. New control signals are calculated by numerical solution of a dynamical optimization problem, with objective to reach stable working conditions. The stress on critical components is calculated and constraints are used to ensure that no components are damaged.

A first model of the Jänschwalde plant to be used for optimization was developed in a previous Vattenfall-based thesis [Andersson, 2013]. The focus of that project was also start-up optimization and this thesis is a direct continuation of that work.

A highly detailed model of the Jänshwalde plant is currently developed at Vattenfall [Hübel et al., 2014]. To optimize this model is however impossible with the tools currently used, as it is far too complex.

Several studies of start-up optimization of combined cycle power plants have been conducted, such as [Casella et al., 2011] and [Lind and Sällberg, 2012]. The latter one is especially interesting as the methods used in that project are the same as for the present one. In [Dietl et al., 2014] the optimization results of a developed version of the model in [Lind and Sällberg, 2012] is presented together with other industrial case studies.

This thesis is conducted within the MODRIO project. MODRIO (Model Driven Physical Systems Operation) is a project with 38 partners in six countries. The aim

of the project is to improve the possibility of using modelling and simulation tools for system operation using open standards [MODRIO].

1.1 Aim of thesis

The starting point of this thesis is the optimization model of the Jämschwalde plant developed by Eva Andersson. The description of this work can be found in [Andersson, 2013]. The main aim of the present thesis is to greatly improve the model and optimization results compared to that project. This aim consists of three parts. The first one is to develop a dynamic model of the plant more suitable for optimization. By doing this, the complexity and tolerances of the optimization, as well as the formulation of the optimization problem should be improved. The second part is to make the model more similar to the real plant by adding and improving components compared to Andersson's model. The third part is to investigate different optimization problem setups and find and compare optimal solutions to the start-up problem. Another aim is to investigate how well suited the current version of the JModelica.org platform is for optimization problems such as start-up optimization of a thermal power plant.

1.2 Structure of thesis

In Chapter 2 the function of a thermal power plant is summarized. The thermodynamics of the steam cycle is presented and the equations used to create a simplified model of the plant are explained. The optimization problem is the focus in Chapter 3. The conversion from a dynamical optimization problem to a non-linear programming problem is explained together with the algorithm used to solve this problem numerically.

In Chapter 4 the programs and tools used in this project are described.

Different aspects of the modelling of the power plant are covered in Chapter 5. A detailed model of the plant is presented, together with key components and modelling features of the simplified optimization model.

Chapter 6 explains the different steps in developing an optimization case which is possible to solve without numerical problems. The specific optimization formulations for the start-up scenario are then presented. The corresponding results can be found in Chapter 7.

The last chapter contains analysis of the results together a discussion of sources of error and possible improvements.

2

Background

In this chapter general theory of coal fired power plants is presented, including the steam cycle, the start-up procedure, and the control system of the plant. The equations that are used for the modelling of the plant are also explained.

2.1 Power plant

Located close to the city of Peitz near the German border to Poland, the Vattenfall owned power plant Jämschwalde is the largest lignite power plant in Germany. The total installed capacity is 3000 GW divided into six blocks [Vattenfall], containing two boilers each. It was built between 1976 and 1988 and has an efficiency of about 36% [Saarinen et al., 2011].

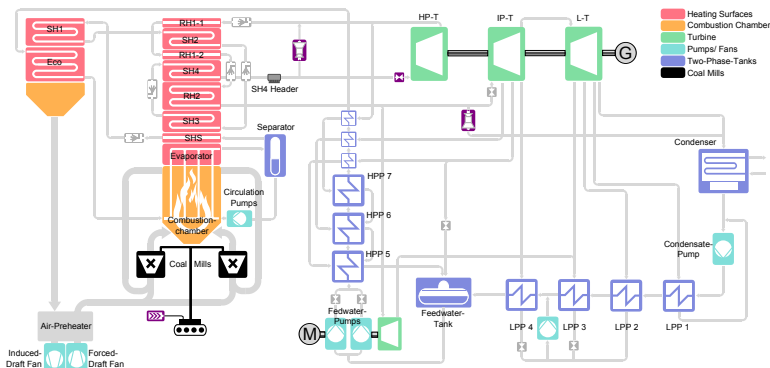


Figure 2.1: Overview of a coal fired power plant. The superheaters and reheaters are denoted SH and RH, respectively, while LPP and HPP are the low pressure and high pressure preheaters. HP-T, IP-T, and L-T are different turbine stages.

A coal-fired power plant converts chemical energy stored in coal to electrical energy. This is done in several steps. By burning the coal hot flue gas is produced. The thermal energy in the gas is used to heat water into steam, which is used to spin a turbine. This mechanical energy is then converted to electricity in a generator.

Steam cycle

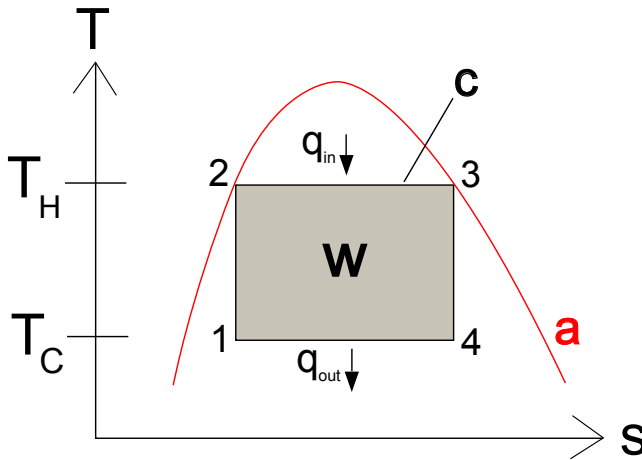


Figure 2.2: T-s (temperature vs entropy) diagram of the Carnot cycle.

For the plant model in this thesis, the most important part of the plant is the steam cycle. Therefore it will be explained in detail below.

An idealized version of the steam cycle in a thermal power plant is the Carnot cycle. This is a thermodynamic cycle, consisting of four stages, where thermal energy is transformed into work. In figure 2.2 the Carnot cycle is illustrated in a temperature-entropy (T-s) diagram. Each point of the curve *c* describes the state of the fluid at a certain point of the cycle, with the steam flow direction being clockwise in the diagram.

Starting from state 1, the fluid is compressed without any exchange of heat with the environment. Next the heat q_{in} is added to the medium at the constant temperature T_H . By expanding the medium isentropically the temperature is then decreased. Finally the fluid is condensed at the constant temperature T_C , while the heat q_{out} leaves the fluid.

In order to add and subtract heat of a medium without changing its temperature it is necessary to conduct the cycle in the two-phase region, meaning that the medium is a mix of liquid and gas. The two-phase region is the area below the curve *a* in figure 2.2. The grey area marked *w* represents the amount of work done over the cycle. Based on this, the efficiency of a Carnot-process can be derived to be

$$\eta = 1 - \frac{T_C}{T_H}. \quad (2.1)$$

This is the highest possible efficiency for a heat engine working in a thermodynamical cycle between the temperatures T_H and T_C [Alvarez, 2006a].

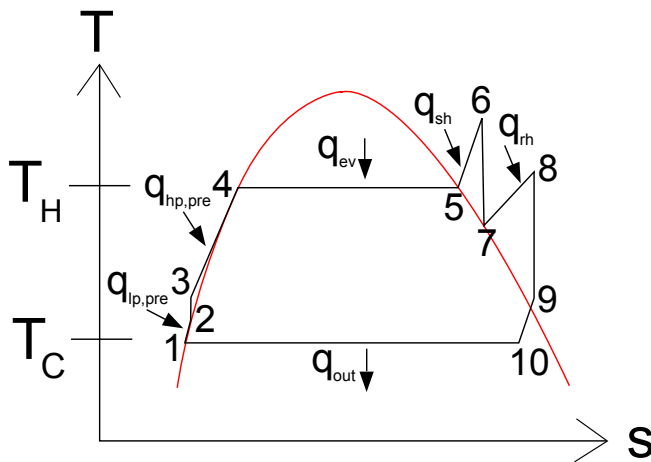


Figure 2.3: T-s diagram of the Rankine cycle with reheat.

The steam cycle in a thermal power plant such as the Jämschwalde plant differs from the Carnot cycle in a number of ways. The Rankine cycle with reheat, illustrated in figure 2.3 is a much better approximation. In table 2.1 the different steps and concepts in the steam cycle are summarized.

In figure 2.1 an overview of a coal fired power plant and its different components can be seen. The economizer, evaporator, superheaters (denoted SH in the figure) and reheaters (denoted RH) are all heat exchangers. They consist of bundles of tubes situated inside the flue gas channel, oriented perpendicular to the gas flow. The evaporator is of particular interest as it is the heat exchanger closest to the furnace. Not all of the coal is yet combusted at this point of the flue gas path, which means that combustion is taking place inside the gas channel. Unlike the rest of the heat exchangers the primary mean of heat transfer in the evaporator is through radiation, whereas convective heat transfer is dominating in the rest of the heat exchangers.

An important component not visible in the Rankine cycle is the separator, situated between the evaporator and the superheaters in the steam cycle. Here liquid water and steam are separated so that only dry steam enters the superheater section. The liquid water is recirculated back through a pump and mixed with the water entering the evaporator.

Step	Rankine cycle process	Real plant location
1 - 2	Heat is added to the fluid	Low pressure preheaters
2 - 3	The fluid is compressed causing an increase in pressure	Feedwater pump
3 - 4	Heat is added to the fluid	High pressure preheaters and the economizer section
4 - 5	By adding more heat the fluid is evaporated	Evaporator
5 - 6	Further heating increases the steam temperature as it gets superheated	Superheater section
6 - 7	The fluid is expanded, while the temperature is decreased and power is generated	High pressure turbine
7 - 8	A second superheating of the fluid	Reheater section
8 - 9	The fluid is expanded while generating power	Low pressure turbine
9 - 10	Heat is taken from the steam to preheat the feed water	Low and high pressure preheaters
10 - 1	To reach the initial state the fluid is condensed completely at constant pressure	Condenser

Table 2.1 The steam cycle of a thermal power plant. The steps refer to figure 2.3.

The superheating is done to increase the efficiency of the process, by increasing the maximal temperature, and to avoid having too moist steam in the turbine, which is damaging. By adding a reheating stage can the evaporation pressure, as well as the temperature at which heat is added, be increased [Alvarez, 2006b]. One should note that also the Rankine cycle is an idealization of the behaviour of a real plant, as for instance the compression and expansion of the steam is not conducted isentropically in reality.

Start-up procedure

Start-up type	Stand-still time	Occurrences in 2012
Hot	$t \leq 12$ h	4
Warm	$12 \text{ h} < t < 48$ h	6
Cold	$t \geq 48$ h	15

Table 2.2 Start-ups of the Jämschalde plant

The start up procedure of the Jämschalde plant is quite time consuming due to two factors. Firstly, there are many processes that need to be initiated slowly in order to avoid damage due to stress on components. Secondly, there is a large

inertia in the system in general. This inertia also means that the amount of time a block has been shut down greatly affects the speed of which it can be restarted. Depending on the stand-still time a start-up procedure is categorized into hot, warm or cold in accordance with table 2.2. The three phases of the start-up procedure will be explained next.

1. Oil burners are used to start the combustion process in the furnace. After starting the coal mills the fuel is gradually changed to coal and the fuel feed is then gradually increased. The pressure is ramped up by the control systems steering different valves. The temperature of the steam as well as the components in the system is increasing until they reach desired values. During this phase the control valves for the different turbine stages are closed while bypass valves are open, so that the steam does not enter the turbine. This phase typically takes around three hours for a cold start.
2. The turbine is accelerated by opening the low pressure control valve slightly. The steam is allowed to enter the low pressure turbine first and later the high pressure. The turbine speed is increased step-wise until it reaches 3000 revolutions per minute. At the same time the bypass valve is closed. The temperature and pressure is increased further. This phase is completed in around four hours.
3. The generator is connected to the electrical grid, while the live steam temperature and pressure is increased as the load reaches its desired value. Full load operation with both boilers running is reached after approximately 18 hours.

In figures 2.4 and 2.5 some key signals during a start-up are plotted for a cold start of block D in the plant conducted the seventh of November 2011. It should be noted that the two boilers of the block are not started simultaneously.

Control system

The control system of the plant consists of several controllers on different levels. Controllers on the higher levels are providing set points for the lower level controllers and on the bottom level actuators and valves are steered. Of significant interest for this project is the separator level control and the live steam pressure control.

The separator level is kept constant by manipulating the feed water flow entering the evaporator. The mass flow affects the separator level indirectly as it decides the steam quality of the water exiting the evaporator. That value is directly coupled to the water level.

Two live steam pressure controllers determines the position of the high pressure control and bypass valves. When the flow needs to be directed through one valve or the other the reference pressures of the controllers are altered so that they do not match, causing one of them to close.

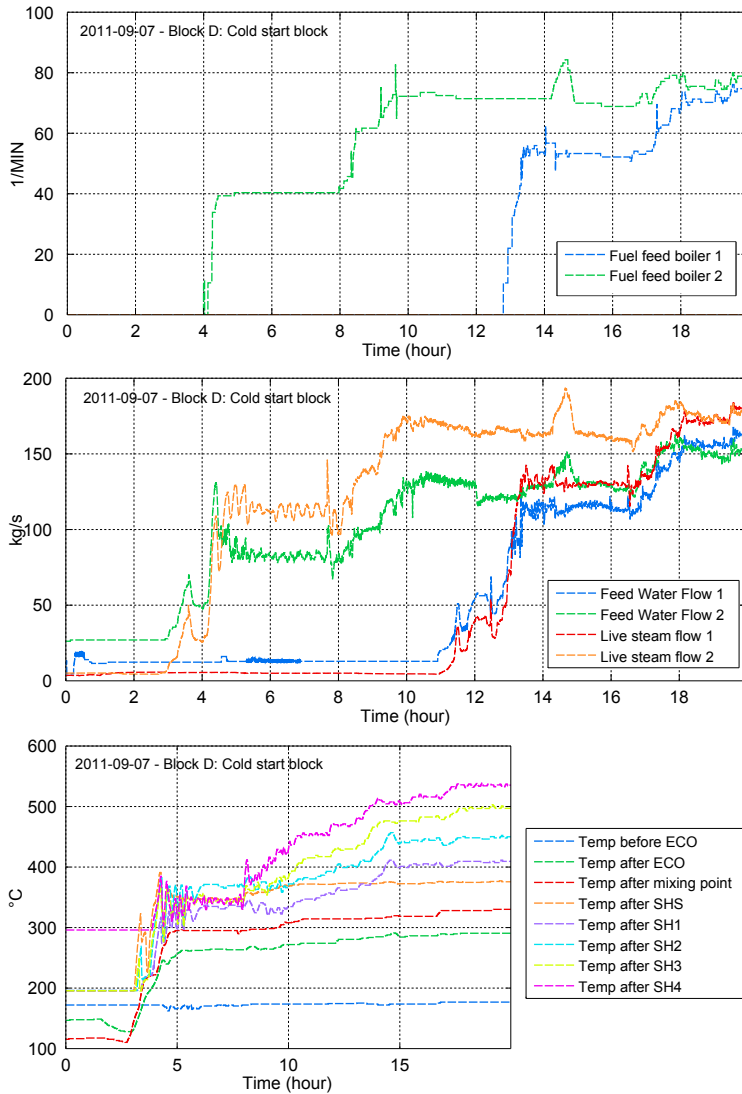


Figure 2.4: Different measured signals during a cold start-up of a block at the Jän-schalwde power plant. Each block has two boilers which are started separately, named 1 and 2 in the legends. On top the coal feeder speed is illustrated, below is the water and steam flow, and the bottom plot shows the steam temperature at different points in the steam cycle.

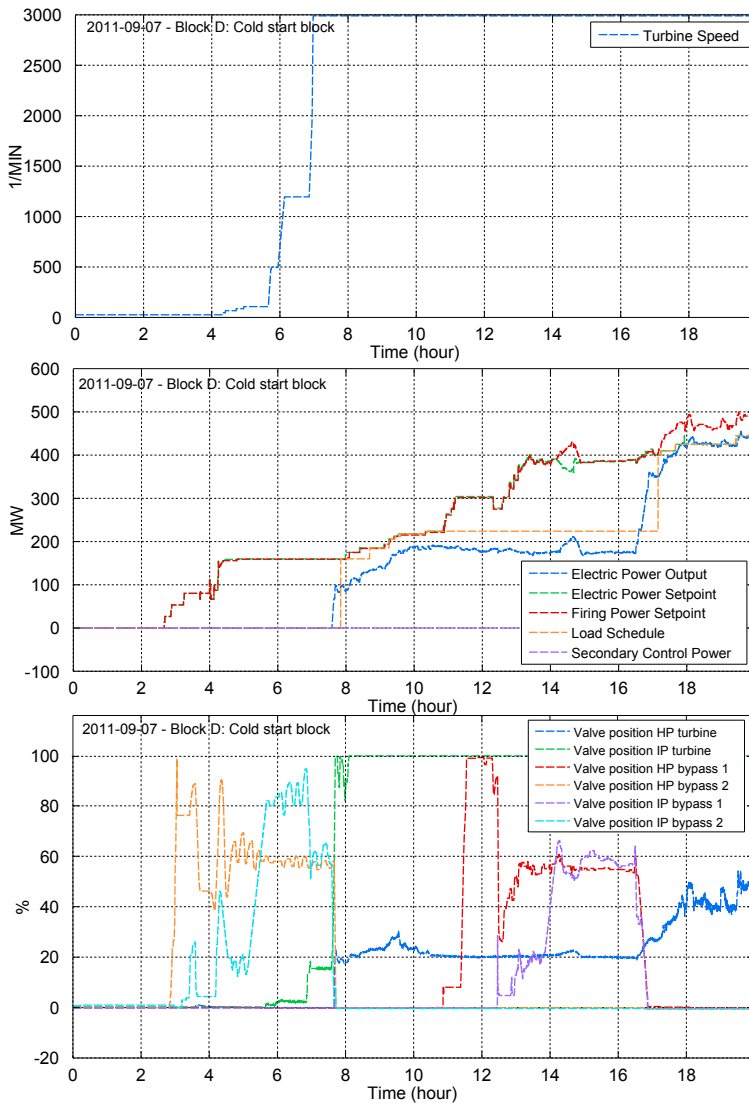


Figure 2.5: The top plot shows the turbine speed. The electric power output is plotted in the middle, together with setpoints and the load schedule, which is a reference signal for the production of the plant. Different valve positions are displayed in the bottom plot. Maximum load is reached after 18 hours.

2.2 Theory

In this section theory regarding the heat exchanger models and stress calculations is presented. The heat exchangers are very important as the heat transfer from flue gas to steam is a central part of the plant model. Furthermore, several of the equations derived for the heat exchangers are also used in other components. Finally, the stress calculations are of great importance as the stress is a major limiting factor during the start-up.

Balance equations

Mass, momentum, and energy balance equations are important in many of the components of the model. The most important ones are the heat exchangers, which will be explained in detail below. The heat exchanger model consists of two volumes connected via a wall with one uniform temperature throughout. Steam is flowing into and out of the volume with the mass flow rates \dot{m}_{in} and \dot{m}_{out} . With positive flow defined as flow into the volume this brings the following expression for the change in steam density ρ

$$\dot{m}_{in} + \dot{m}_{out} = V \frac{d}{dt} \rho. \quad (2.2)$$

The enthalpies h_{in} and h_{out} of the steam flowing into and out of the volume are used to calculate the energy balance in the following way:

$$\dot{m}_{in} h_{in} + \dot{m}_{out} h_{out} + Q_{wall} = V \frac{d}{dt} (\rho u). \quad (2.3)$$

The energy transferred through the media is the product of the enthalpies and their corresponding mass flows. In addition to this there is also an amount of heat $Q_{wall,steam}$ transferred to the wall. The difference between the three forms of energy transfer defines the change in internal energy, which is the product of density and specific internal energy u , of the steam inside the volume. In the gas volume corresponding equations apply, but the internal dynamics are assumed to be neglectable. In practice this means that the derivative terms are replaced with zeroes.

Heat transfer

The heat transfer through the wall depends on the temperature of the wall. The change in wall temperature is determined by equation 2.4, where M_{wall} and c_p are the mass and the heat capacity of the wall, respectively.

$$M_{wall} c_p \frac{d}{dt} T_{wall} = Q_{wall,steam} + Q_{wall,gas} \quad (2.4)$$

The heat transfer between the media and the the wall are calculated using Newton's law of cooling, which for the steam side becomes

$$Q_{wall,steam} = \alpha_{wall,steam} A_{wall,steam} (T_{steam} - T_{wall}) \quad (2.5)$$

$\alpha_{wall,steam}$ is the heat transfer coefficient between the steam and the wall. A corresponding equation is used on the flue gas side. In the optimization model both constant and flow dependent heat transfer coefficients are used. In the flow dependent case the heat transfer coefficient is decided using the Dittus-Boelter equation. This is a relation between the dimensionless Nusselt (Nu), Reynolds (Re), and Prandtl (Pr) numbers. For turbulent flow and cooling of the fluid it reads [Sundén, 2006]

$$Nu = C_1 Re^{C_2} Pr^{C_3}, \quad (2.6)$$

with $C_1 = 0.023$, $C_2 = 4/5$ and $C_3 = 0.3$. The definitions of the different dimensionless numbers now brings the following relation between heat transfer coefficient and mass flow:

$$\alpha = Nu \frac{\lambda}{D} = 0.023 \left(\frac{\rho \dot{m} D}{\mu} \right)^{4/5} \left(\frac{c_p \mu}{\lambda} \right)^{0.3} \frac{\lambda}{D}, \quad (2.7)$$

where λ is the thermal conductivity of the fluid, D is the the hydraulic diameter of the channel, μ is the dynamic viscosity and c_p the heat capacity of the fluid.

The flow dependent heat transfer is used on the flue gas side in all heat exchangers except the evaporator.

Stress calculations

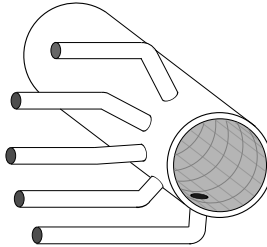


Figure 2.6: Typical header design.

The walls of several components of the plant are considered critical during the start-up schedule of the plant. Therefore we need to calculate the stress in the walls and use constraints on these to prevent damage and shortening of the life length of these components. The separator and the SH4 header are two components assumed to be critical. They both consist of cylindrical pipes connected with smaller pipes (see figure 2.6). The highest stress for these components occur on the edges of the holes at the branching points. To calculate the total stress at these points both the thermal and the mechanical stress must be determined. The mechanical stress is given by

$$\sigma_{ip} = \alpha_m p \frac{d_m}{2s_b} \quad (2.8)$$

Here p is the steam pressure inside the component, d_m is the diameter of the pipe, s_b is the wall thickness and α_m is given by

$$\alpha_m = \alpha_{m0} + f_u \alpha_b, \quad (2.9)$$

where $\alpha_{m0} = 3.2$ and $\alpha_b = 2.0$ are constants determined by the welding of the component and f_u is an unroundness factor which is calculated by the following equation

$$f_u = 1.5 \frac{\frac{d_m}{s_b}}{1 + \frac{1-\nu}{2} \frac{p}{E_\vartheta} \left(\frac{d_m}{s_b}\right)^3} U \quad (2.10)$$

$U = 0.02$ is determined by the variations in diameter of the cylinder, E_ϑ is the modulus of elasticity, and ν is Poisson's ratio for the material. The thermal stress is determined by

$$\sigma_{i\vartheta} = \alpha_\vartheta \frac{\beta_{L\vartheta} E_\vartheta}{1 - \nu} (T_m - T_i). \quad (2.11)$$

Here the form factor $\alpha_\vartheta = 2.0$, $\beta_{L\vartheta}$ is the heat expansion coefficient, and T_m and T_i are the mean and inner temperature of the wall. The total stress is now given by summation:

$$\sigma_i = \sigma_{i\vartheta} + \sigma_{ip} \quad (2.12)$$

Another critical component is the high pressure turbine safety valve, which has a spherical shape. The stress calculations for this component are identical to those for the cylindrical components above, except for equation 2.8, which is replaced with

$$\sigma_{ip} = \alpha_m p \frac{d_m}{4s_b}. \quad (2.13)$$

The operation time of a power plant can be divided into load cycles. For the scenario considered in this thesis only half of a cycle is considered, the start-up. The stress amplitude of a cycle is defined as

$$\Delta\sigma = \frac{\sigma_{max} - \sigma_{min}}{2}. \quad (2.14)$$

The relation between the stress amplitude $\Delta\sigma$, the working temperature, and the life length of a certain component is given by the Wöhler-curve [Meinke, 2012]. In figure 2.7 the Wöhler-curve used for components of the Jämschwalde power plant is displayed for the working temperatures 100°C and 550°C.

It is required that the components of the power plant should withstand 4000 start-ups. Together with the working temperatures, calculated as $0.75T_{max} + 0.25T_{min}$, a maximal stress amplitude can be determined for each component using the Wöhler-curve. This is compared with the maximal stress during a cycle for each component to determine minimum stress constraints. The stress level reaches

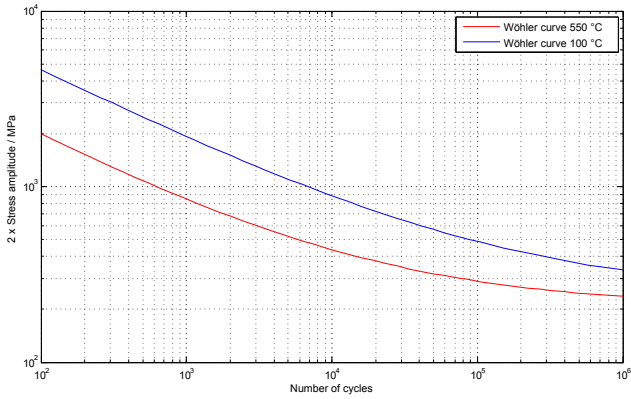


Figure 2.7: Life time calculation using the Wöhler-curve.

its minimal value during the start-up due to the increase in temperature that takes place during this phase. This makes the inner temperature temporarily higher than the mean temperature in the walls, which according to equation 2.11 introduces a negative thermal stress component. As the increase in mechanical stress typically is small compared to the changes in thermal stress a trough in the total stress is therefore created. Figure 2.8 illustrates the relation between the minimal stress value, the maximal stress amplitude, and the stress constraint.

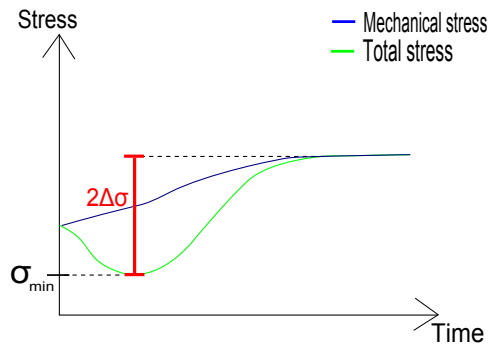


Figure 2.8: Maximal stress amplitude giving minimum stress constraint.

3

Dynamic optimization

Several methods have been developed for solving dynamic optimization problems. The software used in this project uses a simultaneous approach to convert the problem to a large-scale non-linear programming problem, which is solved using an interior point method. More details about this procedure are presented below.

3.1 Differential algebraic equations

The equations which describe our plant model form a generalized system of differential equations called a differential algebraic equation (DAE) system. A DAE system consists of differential equations, such as equation 2.4 and algebraic equations, such as equation 2.5. A general DAE system is as follows

$$F(\dot{x}(t), x(t), u(t), t) = 0 \quad (3.1)$$

where $x(t)$ and F are vectors of variables and functions. The separation $x(t) = (z(t), y(t))^T$, where $z(t)$ is the differential variables and $y(t)$ is the algebraic variables is used to obtain the new formulation

$$F(\dot{z}(t), z(t), y(t), u(t), t) = 0. \quad (3.2)$$

A system of ordinary differential equations can be obtained by differentiating equation 3.2. The number of differentiations needed, n , defines the differential index of the DAE [Ljung and Glad, 2004].

3.2 DAE optimization problem

By combining the DAE system with variable constraints and an objective function, we get a DAE optimization problem. This can be formulated in the following way, in accordance with [Biegler et al., 2001].

$$\min_{z(t), y(t), t_f, p} \varphi(z(t_f), y(t_f), u(t_f), t_f, p) \quad (3.3a)$$

$$\text{s.t. } \frac{dz(t)}{dt} = F(z(t), y(t), u(t), t, p) \quad (3.3b)$$

$$0 = G(z(t), y(t), u(t), t, p) \quad (3.3c)$$

$$z(0) = z^0 \quad (3.3d)$$

$$H_s(z(t_s), y(t_s), u(t_s), t_s, p) = 0 \text{ for } s \in \{1, \dots, n_s\} \quad (3.3e)$$

With the bounds:

$$z^L \leq z(t) \leq z^U$$

$$y^L \leq y(t) \leq y^U$$

$$u^L \leq u(t) \leq u^U$$

$$p^L \leq p(t) \leq p^U$$

$$t_f^L \leq t_f \leq t_f^U$$

where

φ is a scalar objective function,

F are the right hand sides of differential equation constraints,

G are algebraic equation constraints, assumed to be index one,

z are differential state profile vectors,

z^0 are the initial values of z ,

y are the algebraic state profile vectors,

u are the control profile vectors,

p is a time-independent parameter vector,

t_f is the final time.

The objective function is typically on integral form and formulated so that deviations from the desired working conditions for the plant are punished. An example of such a function is

$$\int_0^{t_f} \alpha u^2 + \beta (T - T_{ref})^2 dt \quad (3.6)$$

where α and β are weights deciding how the objectives of keeping u close to zero and T close to T_{ref} are prioritized. Alternatively a minimum time formulation can be used. The constraints introduced in our optimization problem are inequality constraints on control signals and stress levels.

3.3 Non-linear programming

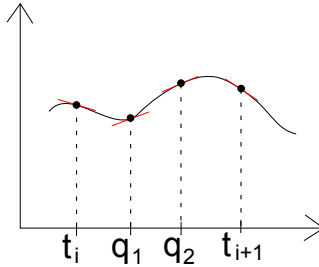


Figure 3.1: An element with two collocation points q_1 and q_2 .

To solve the DAE optimization problem numerically it is converted into a non-linear programming (NLP) problem. This is done through parameterization of state and input profiles by Lagrange polynomials on finite elements. The elements divide the optimization time horizon into smaller sections. For the state profiles a number of Radau collocation points are placed inside each element. The polynomials are chosen so that they match the values and derivatives of the states at each collocation point, see figure 3.1. The last collocation point is placed at the end of the element. The resulting NLP can be formulated in the following way.

$$\min f(x) \quad (3.7a)$$

$$\text{s.t. } c(x) = 0 \quad (3.7b)$$

$$x^L \leq x \leq x^U \quad (3.7c)$$

3.4 Interior point method

We assume that the inequality constraints of 3.7 are on the form $x \geq 0$. If they are not this can be achieved by variable substitution and introduction of slack variables. To solve the NLP we will then introduce the following barrier problem.

$$\min \varphi_\mu(x) = f(x) - \mu \sum_{i=1}^n \ln(x^{(i)}) \quad (3.8a)$$

$$\text{s.t. } c(x) = 0 \quad (3.8b)$$

where μ is a barrier parameter greater than zero. As the logarithmic function grows towards infinity when x goes to zero the solution to this problem will always be in the interior of the set $\{x|x \geq 0\}$. For this reason the inequality constraint can be removed. By letting μ go to zero the solution to 3.8 will converge to the one of 3.7. For each value of μ the barrier problem is solved using the Karush-Kuhn-Tucker optimality conditions. These are first order necessary optimality conditions, which for the barrier problem according to [Biegler et al., 2001] becomes

$$\nabla f(x) + \nabla c(x)y - z = 0 \tag{3.9a}$$

$$c(x) = 0 \tag{3.9b}$$

$$XZe - \mu e = 0 \tag{3.9c}$$

$$x, z \leq 0, \tag{3.9d}$$

where

$\nabla f(x)$ is the gradient of the objective function,

$\nabla c(x)$ is the gradient of the constrains,

y are the Lagrange multipliers for the equality constraints,

z are the Lagrange multipliers for the bound constraints,

Z is a diagonal matrix with the elements of z ,

X is a diagonal matrix with the elements of x ,

p is a time-independent parameter vector,

e is a vector of ones.

Newton's method is used to find a solution to this system of nonlinear equations. To verify that the found solution indeed is a minimum a method called Hessian regulation is used [Wächter, 2009].

4

Programs and tools

The two main tools used in this project are Dymola and JModelica.org. Dymola is a commercial program for creating and simulating models written in the language Modelica, while the open source platform JModelica.org is used for simulation and optimization of Modelica and Optimica models.

4.1 Modelica and Dymola

The models developed within this project are written in the equation based language Modelica. It is a free standardized language where differential, algebraic, and discrete equations can be used to describe the models in an object-oriented way. The main class in the language is the `model` class. Parameters and variables are defined in the model and in the `equation` section the relation between these are defined. A simple Modelica model from [*JModelica.org User's guide 2014*] is displayed below.

```
model VDP
  // State start values
  parameter Real x1_0 = 0;
  parameter Real x2_0 = 1;

  // The states
  Real x1(start = x1_0);
  Real x2(start = x2_0);

  // The control signal
  input Real u;

  equation
    der(x1) = (1 - x2^2) * x1 - x2 + u;
    der(x2) = x1;
end VDP;
```

Variables can have several attributes. Some of the most important ones are `start`, `fixed`, `nominal`, `min`, and `max`. With `min` and `max` a range for a variable can be

defined. The `nominal` attribute represents a nominal value used as a scaling factor to improve numerical properties. If the attribute `fixed` is set to `true`, the initial value of a variable is given by the `start` attribute. An alternative way to define initial values for the variables is provided by the `initial equation` section.

Dymola is a commercial program offering a modeling environment and a Modelica translator, used to transform the Modelica code into C-code which in turn is used for simulating the model. In the modeling environment models can be created and navigated in both the text view, showing the Modelica code, and the diagram view, which is a graphical interface.

The typical way to use Dymola when creating a complex models is to arrange and connect components in the graphical view in a way corresponding to the system one wants to represent. The connection lines represents the physical coupling between the components and a connector class is used to describe the equations corresponding to the connection. The components can be found in different libraries, such as the open-source Modelica Standard library or commercial ones like the Thermal power library from Modelon, but it is also possible to construct components of your own using Modelica code.

4.2 Optimica

Optimica is an extension of the Modelica language used for dynamic optimization of Modelica models. The main feature of it is the new specialized class `optimization`, within which the optimization problem to be solved is defined. The attributes `objective`, `startTime`, `finalTime`, and `static` are added to the optimization class. `objective` defines the type of objective function which should be used while `startTime` and `finalTime` define the boundaries in time for the optimization problem. Another key element is the `constraint` section where equality, inequality, and point constraints can be defined. However these can also be defined using the `min` and `max` attributes described in the previous section. For more information about Optimica, see [Åkesson et al., 2010].

4.3 JModelica.org

The open source platform JModelica.org has been used mainly for optimization, but also simulation during the project. The optimization problem is solved by translating it into a non-linear programming (NLP) problem. This is conducted by parameterizing the state and input profiles by Lagrange polynomials [Åkesson et al., 2010] as explained in Chapter 3. The user interaction with the platform is done with the scripting language Python. Three different types of model objects can be created in JModelica.org: `FMUModel`, `JMUModel`, and `CasadiModel`. As the platform for using `CasadiModel` was still under development during the the time the thesis was conducted only the first two were used during this project.

Simulation

When simulating a model from the JModelica.org environment an `FMUModel` is typically used. To create such a model a functional mock-up unit (FMU), which is a compressed file following the FMI standard [FMI], is needed. The FMU is created by compiling Modelica models, either in JModelica.org, or in some other tool that support FMU export. The reason for using FMUs rather than JMUs for simulation is that the DAE of the model is converted into an ODE in the FMU, which results in better performance [JModelica.org User's guide 2014]. For further information about the handling of FMU:s in JModelica.org see [Andersson et al., 2011]. The python commands used for compiling a Modelica model, loading the FMU and simulating the resulting `FMUModel` are displayed below.

```
from pymodelica import compile_fmu
from pyfmi import load_fmu

fmu_name = compile_fmu("MyModel", "MyModel.mo")
simMod = load_fmu(fmu_name)
simRes = simMod.simulate(final_time=1000)
```

Optimization

Similar to the FMU, a JMU (JModelica.org model unit) is a compressed file which can be created through compilation of a Modelica model in JModelica.org. However JMUs can also be, and usually are, created by Optimica models, as they are typically used for optimization. By loading a JMU in JModelica.org a `JMUModel` is created. The following code displays how the optimization of an Optimica model is conducted.

```
from pymodelica import compile_jmu
from pyfmi import JMUModel

jmu_name = compile_jmu("MyModel", "MyModel.mop")
optMod = JMUModel(jmu_name)
optRes = optMod.optimize
```

IPOPT

The open-source software package IPOPT [IPOPT] is used to solve the non-linear programming problem created by JModelica.org. It uses the interior point method described in Chapter 3 and is suitable for large-scale problems. The solver produces output during each step of the iterative optimization procedure, a typical example of this can be seen in figure 4.1. Each row corresponds to one step in the iteration, while information such as step sizes, infeasibilities, and the value of the objective function at each step can be found in the different columns. By interpreting this output information about how to improve the optimization model can be gained.

```

*****
This program contains Ipopt, a library for large-scale nonlinear optimization.
Ipopt is released as open source code under the Eclipse Public License (EPL).
For more information visit http://projects.coin-or.org/Ipopt
*****
This is Ipopt version 3.10.3, running with linear solver ma27.

Number of nonzeros in equality constraint Jacobian...:    4104
Number of nonzeros in inequality constraint Jacobian.:    0
Number of nonzeros in Lagrangian Hessian.....:          0

Total number of variables.....:    1258
   variables with only lower bounds:          0
   variables with lower and upper bounds:    122
   variables with only upper bounds:          0
Total number of equality constraints.....:    1139
Total number of inequality constraints.....:    0
   inequality constraints with only lower bounds:    0
   inequality constraints with lower and upper bounds: 0
   inequality constraints with only upper bounds:    0

iter   objective      inf_pr   inf_du lg(mu)  |d|| lg(rg) alpha du alpha_pr ls
0 5.0019416e+001  6.61e+000  1.18e-002  0.0 0.00e+000 - 0.00e+000 0.00e+000 0
1 3.172667e+001  4.44e+000  1.04e+000 -5.0 2.31e+001 - 0.07e-001 1.00e+000f 1
2 3.9909131e+001  2.48e-001  4.21e-002 -6.0 8.20e+000 - 9.39e-001 1.00e+000h 1
3 3.9977724e+001  1.48e-001  2.28e-002 -2.8 2.17e+000 - 9.95e-001 1.00e+000h 1
4 4.0110574e+001  8.72e-002  1.46e-002 -4.5 5.81e-001 - 9.91e-001 1.00e+000h 1
5 4.0023952e+001  3.90e-001  9.19e-003 -5.2 1.26e+000 - 1.00e+000 1.00e+000h 1
6 4.0055303e+001  4.10e-002  1.66e-002 -6.7 5.39e-001 - 1.00e+000 1.00e+000h 1
7 4.0070413e+001  1.28e-002  1.79e-003 -8.1 2.95e-001 - 1.00e+000 1.00e+000h 1
8 4.0081169e+001  2.72e-004  1.48e-003 -10.0 3.70e-002 - 1.00e+000 1.00e+000h 1
9 4.0081034e+001  4.84e-003  9.85e-004 -11.0 1.22e-001 - 1.00e+000 1.00e+000h 1
iter   objective      inf_pr   inf_du lg(mu)  |d|| lg(rg) alpha du alpha_pr ls
10 4.0081001e+001  4.16e-004  1.14e-003 -11.0 4.57e-002 - 1.00e+000 1.00e+000h 1
11 4.0081069e+001  1.03e-003  8.00e-005 -11.0 6.14e-002 - 1.00e+000 1.00e+000h 1
12 4.0081116e+001  4.60e-007  3.49e-005 -11.0 2.21e-003 - 1.00e+000 1.00e+000h 1
13 4.0081116e+001  6.94e-000  0.94e-006 -11.0 1.17e-003 - 1.00e+000 1.00e+000h 1
14 4.0081116e+001  7.96e-009  1.73e-006 -11.0 2.26e-004 - 1.00e+000 1.00e+000h 1
15 4.0081116e+001  4.43e-008  6.29e-007 -11.0 5.34e-004 - 1.00e+000 1.00e+000h 1
16 4.0081116e+001  1.54e-007  6.86e-007 -11.0 9.52e-005 - 1.00e+000 1.00e+000h 1
17 4.0081116e+001  2.26e-009  1.45e-000 -11.0 1.23e-004 - 1.00e+000 1.00e+000h 1
18 4.0081116e+001  2.39e-010  9.34e-009 -11.0 1.61e-006 - 1.00e+000 1.00e+000h 1

Number of Iterations....: 18

                                (scaled)                (unscaled)
Objective.....:    4.008116040428917e+001    4.008116040428917e+001
Dual infeasibility.....:    9.3446605280156358e-009    9.3446605280156358e-009
Constraint violation.....:    9.0629470177292824e-013    2.3283064365386963e-010
Complementarity.....:    1.0000000000000003e-011    1.0000000000000003e-011
Overall NLP error.....:    9.3446605280156358e-009    9.3446605280156358e-009

Number of objective function evaluations = 19
Number of objective gradient evaluations = 19
Number of equality constraint evaluations = 19
Number of inequality constraint evaluations = 0
Number of equality constraint Jacobian evaluations = 19
Number of inequality constraint Jacobian evaluations = 0
Number of Lagrangian Hessian evaluations = 0
Total CPU secs in IPOPT (w/o function evaluations) = 0.125
Total CPU secs in NLP function evaluations = 0.015

EXIT: Optimal Solution Found.

Total time: 0.20 seconds
Initialization time: 0.01 seconds
Solution time: 0.19 seconds
Post-processing time: 0.00 seconds

```

Figure 4.1: IPOPT output

Information about the algorithms implemented in IPOPT can be found in [Wächter, 2009].

5

Modelling

The optimization model is created in Dymola. The structure of it is based on the model created by [Andersson, 2013], but the components have been altered in several ways. Firstly, the units in all the components and the selected states in most of them have been changed in order to make the complete model more optimization friendly. Secondly, the heat transfer model in the heat exchangers has been improved by the introduction of flow dependent heat transfer coefficients. There are furthermore several new components and connections to describe the behaviour of the real plant better.

5.1 Detailed model

A highly complex model, attempting to describe the Jänschwalde plant and its control system in a very detailed fashion, is developed in a collaboration between Vattenfall and Rostock University. Due to its high complexity it is not possible to use this model for optimization purposes. It is instead used as a reference for model structure and parameters values. An overview of this model is displayed in figure 5.1. Details about this project can be found in [Hübel et al., 2014].

5.2 Media models

It is of great importance that the media properties of water at different pressures and temperatures are implemented in the model with high accuracy. There are standard water media models implemented in Modelica libraries for this purpose, but these are not suitable for optimization. Therefore a library developed by Modelon AB called *Water_Poly* is used instead. This library contains functions to determine water properties such as temperature. The functions are polynomial approximations of standard water property functions, with enthalpy and pressure as typical inputs. More details about this method to model water in two-phases can be found in [Bauer, 1999]. For the flue gas no such model exists, instead constant parameters are used to model the properties.

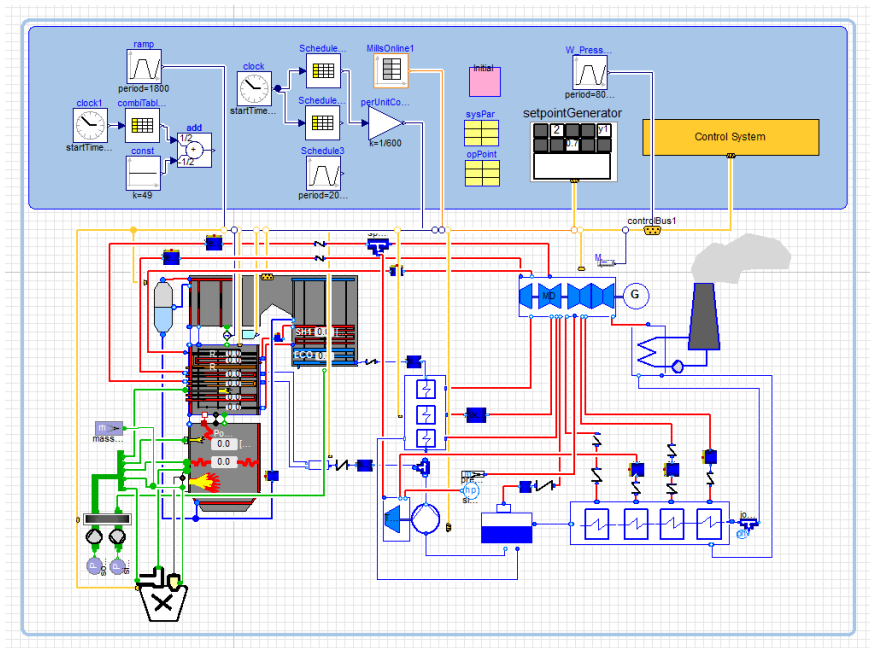


Figure 5.1: Overview of the detailed plant model in Dymola.

5.3 Start-up optimization model

The optimization model of the Jämschwalde plant can be seen in figure 5.2. Many of the key features of the steam cycle, explained in Chapter 2 are represented in this model, as well as some thick-walled components where stress is calculated and two control loops. The model contains 260 equations and 40 states. The biggest structural simplification of the optimization model is that a large part of the steam cycle is replaced with boundary conditions. The non-modelled parts include the preheater and economizer section and the low pressure turbine. Parts that are highly simplified are the coal mill and furnace, they are replaced with a simple gas source.

The most important components of the model are described below.

Evaporator, superheaters and reheaters

The superheaters and reheaters are together with the evaporator the most important parts of the plant model. They are all heat exchangers with flow-dependent heat transfer coefficient on the gas side, except for the evaporator, where a constant heat transfer coefficient is used. Each heat exchanger contains three states; two describing the steam, where the entire volume is lumped into one element, and one for the wall, which also is assumed to have the same temperature throughout and is separating the steam and the gas.

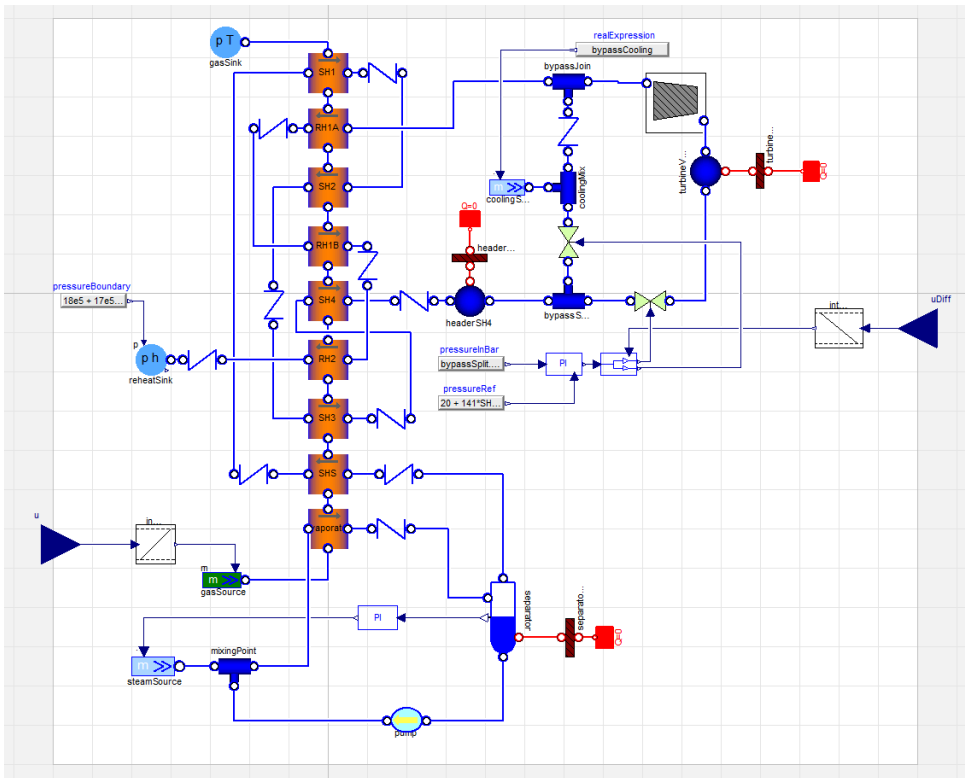


Figure 5.2: The optimization plant model.

Header and high pressure safety valve

These components are modelled using a volume with a wall component attached to it. Stress on the wall is calculated using the equations described in Chapter 2. The walls are parametrized using three nodes in order to determine the mean temperature.

Pressure drop model

"Valves" are used to model the steam pressure drops that take place in the plant. They are all assumed to be linear and are situated in between other components. For all other components (except the turbine) the steam pressure is the same at inlet and outlet.

For the turbine bypass and pressure control loop, valves with variable conductivity are used. These are used both to direct the steam flow and to control the pressure in the system.

Turbine

In the turbine component the steam pressure and enthalpy is decreased in accordance with Stodola's law, a standard way to model steam turbines. It is a static model where the mechanical power output is calculated based on the mechanical and isentropic efficiencies.

Separator

In the separator the incoming water is separated into dry steam and liquid water. During normal operation two-phase water is entering the separator. The water leaving the blowdown at the bottom is then assumed to be saturated liquid while the water exiting the drain is saturated steam. Balance equations are used to determine the water level. It has a wall component with stress calculation attached to it just like the header.

PI controller

Control loops are used in two places in the plant model; the separator level control and the live steam pressure control. The PI controller without anti-windup is chosen due to its simplicity, rather than to match the control system of the real plant exactly. For the separator level control the PI controller is implemented in a standard fashion.

For the live steam pressure control this is not possible as there are two valves that should determine both the live steam pressure and in which direction the steam should flow. Therefore a solution with one controller manipulating both valves is used. An extra input is used to decide how the flowing steam is divided between the two routes. The following equations determine how the signal from the controller affects the valves.

$$o_{bp} = \frac{\lambda}{100}y \quad (5.1a)$$

$$o_{turb} = \frac{100 - \lambda}{100}y \quad (5.1b)$$

where y is the signal from the controller, o_{bp} and o_{turb} are the levels of opening for the bypass and turbine valve respectively, and λ the extra input deciding the relation between the valve openings. In this way each of the valves can be used for pressure control, but also be closed while the other keeps the pressure.

Pump

An ideal pump model is used to create a constant flow from the blowdown of the separator. It fixes the mass flow through it to a user defined value and the pressure of the steam is built up in the pump to correspond with this mass flow. The enthalpy is assumed to be constant.

5.4 Units

For the optimization to work properly all important variables need to be properly scaled. In Modelica nominal values are used for this purpose. A method that simplifies the effort to make sure that all variables are properly scaled is to use units, which are predefined types in the Modelica environment. Units also have the added benefit of an automatic check that the equations formulated in the model are physically consistent. For our plant model new unit types were created. Like the units of the *Water_Poly* library these are extensions of the of the standard SI-units, but with nominal values chosen specifically to fit the conditions in our model. The method for deciding these values is described in Chapter 8.1.

5.5 Boundary conditions and model simplifications

As a significant part of the steam cycle is missing in the optimization plant and the control system is highly simplified, several boundary conditions must be added to this model. These conditions and how they have been determined are presented below.

Reheat pressure boundary

In the real plant the reheat steam pressure is decided by the low pressure turbine and bypass valves just like the high pressure turbine and bypass valves in the optimization plant. As the low pressure turbine system is not added in the optimization model a pressure source is used instead. The profile for the pressure should ideally be treated as optimization input, but to simplify the optimization predetermined expressions were used instead. For phase 1 a linear dependency between the pressure and the steam mass flow was assumed, based on the pressure profiles of a cold start in the power plant handbook [*Kraftwerk Jämschwalde* 2012]. For phase 2 a constant value of 18 bar was used.

Flue gas enthalpy

The flue gas enthalpy was chosen so that the SH4 output temperature in the optimization model matched the real plant at full load. To account for the fact that the gas enthalpy is decreased for lower loads a linear dependency between gas mass flow and enthalpy was assumed in accordance with equation 5.2, where the parameter values $a=1342000$ and $b=1005$ were chosen so to achieve a reasonable live steam temperature for lower loads.

$$h = a + b \cdot \dot{m} \quad (5.2)$$

Live steam pressure

During phase 2 the live steam pressure is not used as input for the optimization, which is the case for phase 1. The reason for this is to reduce complexity of the

optimization problem. To obtain a ramping of the pressure during this phase a linear dependency between live steam pressure and mass flow is assumed, so that the initial and final pressure match the values from the real plant for this phase.

5.6 Calibration

Since the optimization model is highly simplified the behaviour of this plant model will not match the real plant exactly. However, to make the model as similar to the real plant as possible, certain parameter values can be modified in order to minimize the error. Ideally this task would be solved as an optimization problem, which could be handled by an optimization platform such as JModelica.org. A suitable technique for which a suitable set of free parameters and the optimal values of these would be grey-box identification, details about how this method can be implemented in JModelica.org can be found in [Palmkvist, 2014]. To develop and solve such an optimization problem is however not in the scope of this thesis. Therefore the parameters are modified manually until a reasonable similarity between model and measurement is reached.

Heat transfer parameters

The most important experimentally determined parameter values are the heat transfer coefficients of the heat exchangers in the model. For each heat exchanger these were matched with data from the detailed plant model. However for the evaporator this was not possible as the evaporator of the detailed model is modelled differently compared to other heat exchangers. In the detailed model the main form of heat transfer is radiation, which together with recirculation of flue gas and coal combustion inside the component makes it very hard to compare the two models directly. Therefore the heat transfer parameters of the evaporator were chosen so that the entire system would match data from the detailed model.

Validation

For the heat transfer parameter values of the superheaters and reheaters the values from the detailed model were used as initial guesses. Cases were created for each heat exchanger with identical input signals (mass flow rates, pressures and so on) as the corresponding heat exchanger in the detailed model the and the corresponding output signals were compared. Based on this parameter values were altered so that the signals matched to a reasonable degree.

For the water side mean values of the variable heat transfer coefficients in the detailed model were used and they typically were not altered a lot. For the gas side mean values of the different heat transfer parameters were used. The C_1 parameter of equation 2.6 was then altered to reach good matching for each component. Furthermore, the choice $C_3 = 0.4$ was used throughout the model, despite that this is not the nominal value, as it seemed to get a better fit. A comparison between the

Component	$\alpha_{wall,steam} / \text{W}/(\text{m}^2 \text{ K})$	$\alpha_{wall,gas} / \text{W}/(\text{m}^2 \text{ K})$	C_1	$\mu / \text{Pa s}$	$\lambda / \text{W}/(\text{m K})$
Evaporator	12000	195			
SHS	4500		0.11	$5.0 \cdot 10^{-5}$	0.092
SH1	1800		0.25	$3.2 \cdot 10^{-5}$	0.053
SH2	2819		0.077	$3.8 \cdot 10^{-5}$	0.065
SH3	5600		0.066	$4.6 \cdot 10^{-5}$	0.084
SH4	3896		0.068	$4.2 \cdot 10^{-5}$	0.072
RH1A	2300		0.092	$3.7 \cdot 10^{-5}$	0.063
RH1B	1800		0.105	$4.0 \cdot 10^{-5}$	0.069
RH2	2200		0.074	$4.4 \cdot 10^{-5}$	0.078

Table 5.1 Heat transfer parameter values.

output of a heat exchanger from the detailed model and the optimization model can be seen in figure 5.3, where the input gas mass flow (between 800 and 900 s) and temperature (between 1200 and 1300 s) are ramped in separate stages. For the time span 1000 to 1200 s the best fit can be observed, which is expected as this is the working conditions which the chosen parameters values have been based on. In the final phase of the simulation there is a difference between the steam temperatures. The constant gas heat transfer properties not being accurate for this temperature could be a possible explanation for this.

For the evaporator the amount of transferred heat decides the water mass flow

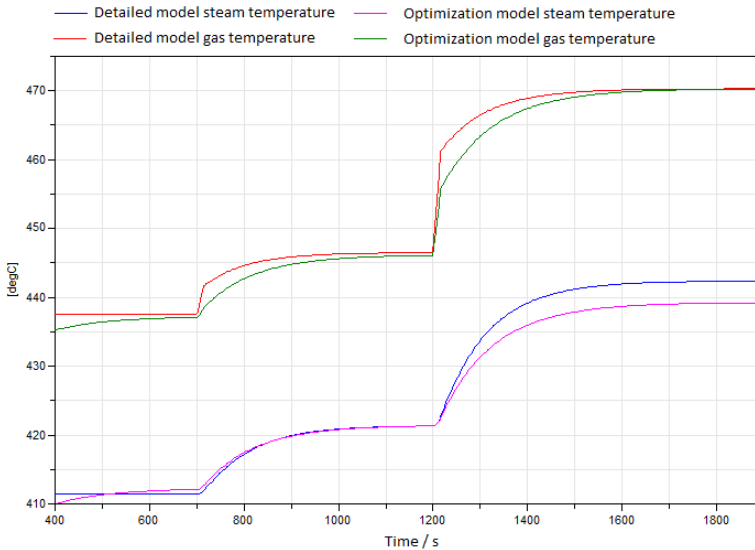


Figure 5.3: Gas and steam output temperatures for superheater 1. The input gas mass flow and temperature are ramped in two separate stages.

Component	$T_{steam,detailed} / ^\circ\text{C}$	$T_{steam,opt} / ^\circ\text{C}$	$T_{gas,detailed} / ^\circ\text{C}$	$T_{gas,opt} / ^\circ\text{C}$
Evaporator		357.8	1136.5	844.9
SHS	357.9	354.9	1119.2	834.8
SH1	423.3	422.8	448.2	465.4
SH2	458.7	466.7	663.9	670.1
SH3	504.0	501.0	972.8	812.0
SH4	535.2	537.1	779.1	785.8
RH1A	394.8	398.1	615.4	621.5
RH1B	485.0	480.5	717.3	724.2
RH2	540.0	532.5	871.1	813.4

Table 5.2 Full load heat exchanger temperature comparison.

indirectly through the separator level control. Therefore this value, together with the gas enthalpy, was used to match the water mass flow and the superheater 4 water output temperature to the corresponding values for a high load scenario of the detailed model.

The chosen heat transfer parameter values for all heat exchangers are summarized in table 5.1. The steam and gas temperatures during a high load simulation of the detailed plant model and the optimization model are summarized in table 5.2.

For full load operation it can be noted that the steam temperatures match the detailed plant with a precision of around 5°C for all heat exchangers, while very large temperature differences can be noted on the gas side. No heat transfer through radiation and missing heat transfer in between the modelled heat exchangers are probably the main causes for this behaviour. The simplified modelling of the flue gas properties could also be contributing to this error. However, as the steam cycle is much more important than the behaviour of the flue gas, the mismatch in temperatures on the gas side is acceptable.

6

Optimization

In order to create an optimization friendly model, a large part of the total time invested in this project was spent investigating very simple models and optimization cases, compared with the full plant model. The aim of this approach was to identify components and parameters critical for the performance of the optimization algorithm and to handle the possible problems as early as possible. In the simplified models this task is much simpler than for the full plant, since the amount of parameters and variables is much higher there. When the optimization of the simplified models worked satisfactorily, the model complexity was gradually increased with new components. At the same time more challenging optimization cases were tried.

6.1 Building an optimization model

The first optimization case considered was to reach a certain steam temperature for one heat exchanger with the derivative of gas mass flow or temperature as input. The next step was to introduce a volume component with a wall with stress calculations. A constraint on the stress level was introduced in the optimization formulation. The effects of adding more heat exchangers and an additional volume were then investigated. The number of components in the model was increased until a model topologically identical with the one created by [Andersson, 2013] was reached. Finally, new components and connections were added to achieve a more realistic plant model.

Setting selection

While investigating simple optimization cases several optimization settings were decided based on various tests. These choices were then used throughout the rest of the project. A presentation of the most important decisions can be found below.

States The formulation of the thermodynamical equations affects how suitable the model is for optimization. For this reason a different set of states was chosen in the new components compared to Andersson's model. Instead of pressure and enthalpy

as states, density and internal energy were chosen. By doing this partial derivatives which in general takes on very small values were eliminated from the formulation.

By comparing the two different sets of states it can be observed that the choice density and internal energy leads to better performance during optimization. The difference is especially visible when variable scaling is not used. With pressure and enthalpy as states does scaling of the critical partial derivatives increase the convergence speed significantly, but it is still worse than for the density and internal energy state selection.

It can however not be said that it is always better to use density and internal energy as states. If the water in a component mostly is in liquid phase could pressure and enthalpy be more suitable, as the in this case the changes in density are very small.

Scaling The choice of nominal values for variable scaling can be complicated as it is not necessarily better to scale down all variables to a magnitude around one, since the variation of the variable also needs to be considered. A better strategy is to base the scaling on the standard deviation of a variable, but this can vary between different components and optimization cases. Therefore different sets of scaling for the different variables were tried and the setup with the best optimization convergence was chosen. The nominal values were in general introduced through the units of the variables. To cope with variables with the same unit taking different values extra units have been added in some instances.

Equation scaling have been necessary in two cases; in stress calculation equations and equations describing the total internal energy in volumes. In both these cases the large magnitude of the terms in the equations caused simulation problems. It has not been used otherwise.

Constraint formulation The constraints in a model are handled differently depending on if they are formulated as variable attributes or in the separate constraint section, described in chapter 4.2. For the simple models no difference was observed between the two alternatives. However, for more complex models the optimization performance was clearly superior with the constraints as attributes.

A method where all min and max attributes introducing inactive constraints in the model were removed, was tried. This idea had proven successful in another project and it did affect the optimization convergence for this model too, but it did in general not improve the convergence speed.

Tolerance When optimizing models with steam pressures higher than approximately 100 bar it proved necessary to increase the tolerance from the default value in the optimization settings. The higher pressure apparently makes it harder to obtain solutions satisfying both optimality and the model equations with very small errors, which can be explained by the increased pressure makes the relative tolerance smaller.

Component	σ_{max} / MPa	T_{min} / °C	T_{max} / °C	$\Delta\sigma$ / MPa	σ_{min} / MPa
SH4 header	97.5	246	537	346	-595
HP safety valve	35.3	240	527	353	-671
Separator	682	195	355	456	-230

Table 6.1 Critical component stress level calculations.

Convergence affecting components

The component causing the most difficulties during optimization was the separator. It is based on a component from the thermal power library, but altered to fit the optimization model. The key modifications for getting the optimization to work with the separator model included were exchanging a spline function from a hyperbolic to a polynomial function and improving the variable scaling for the water mass. The importance of scaling for the separator can be explained by the large volume of liquid water this component contains, which makes the water mass much larger than in other components. The liquid water also makes the selected states of density and internal energy less suitable as explained in the states section above. The introduction of a pump connected to the blowdown might also have had a positive result.

It was anticipated that introducing control loops in the model would complicate the optimization problem, as a fast start-up would require well trimmed loops. This was however not observed during this project.

6.2 Constraint calculation

The constraints used in the optimization problem are very important as they define boundaries for the operation of the plant.

Stress constraints

Simulations give the maximal stress levels for each of the critical components and their working temperatures. These are summarized in table 6.1, together with the maximal stress amplitudes, which are calculated with the Wöhler-curve based on the temperatures. The corresponding minimum stress constraints can also be found in the table, calculated in accordance with figure 2.8.

Flue gas mass flow

The speed of which the flue gas mass flow can be increased or decreased is also constrained. To approximate how fast it is allowed to change simulation data from the detailed plant model is used. By examining the changes in gas mass flow when the plant switches between different loads a constraint of $\pm 0.15 \text{ kg/s}^2$ is derived. However, as this empirical value might not be the actual limit for the plant constraints of $\pm 0.26 \text{ kg/s}^2$ and $\pm 0.5 \text{ kg/s}^2$ are also tried.

Pressure set point

It also proved necessary for optimization purposes to constraint how fast the live steam pressure setpoint could be changed. As it is not known how fast changes are feasible in the real plant a value of ± 0.03 bar/s was chosen.

Valve opening ratio

The constraints on the speed of valve opening ratio changes are chosen so that they in general do not get active. The exception is cases where only monotonous ratio changes are allowed, then the minimum constraint is set to zero.

6.3 Optimization cases

To simplify the optimization formulations the start-up scenario was split into two phases roughly corresponding to the last part of phase one and entire phase two of the start-up of the real plant.

Phase 1

For phase 1 the temperature and pressure profiles are optimized with the live steam controller pressure setpoint and the gas mass flow as input. Deviations from objective live steam pressure and temperature are included in the cost function as well as the control signals. Minimum constraints are used on the wall stress of the SH4 header and the separator. The turbine valve is closed during this phase and the whole turbine section is therefore removed from the model. The initial live steam pressure and gas mass flow of the optimization scenario are chosen to be 15 bar and 26 kg/s. The desired live steam pressure and temperature are 80 bar and 618 K, respectively.

Phase 2

In this phase the objectives are an increased live steam temperature and bypass valve closing. The live steam pressure is chosen to be linearly dependent on the live steam mass flow and is therefore also increased. A stress constraint on a safety valve in the turbine steam route is added, which prevents the bypass valve from closing immediately. The start of the optimization scenario matches the final conditions of phase 1, with a live steam pressure of 80 bar and a gas mass flow of 100 kg/s. The goal of this phase is to reach a live steam temperature of 808 K, with a corresponding live steam pressure of 121 bar.

6.4 Initialization

In order to find a solution to the NLP problem the optimization algorithm is dependent on a good initialization. In this project an initial trajectory was created by simulating the optimization model. The model was typically simulated twice, with

Option	Chosen value	Comment
Mu strategy	Adaptive	
Number of elements	10-16	Depending on optimization case
Tolerance	$5 \cdot 10^{-6}$	
Acceptable tolerance	$3 \cdot 10^{-5}$	
Blocking factors	Ones	Control signal constant over each element

Table 6.2 Optimization solver options

the first results being discarded in order to avoid fast transients during the first part of the optimization. The initial values for the optimization and the initial trajectories were then taken from the second simulation. For phase 2 a steady state initial trajectory with all inputs at zero proved sufficient to obtain good convergence for the optimization algorithm. For phase 1 constant non-zero inputs for both control signals were used during initialization, bringing the system closer to the desired state for the final time than zero inputs would do. It proved hard to achieve convergence of the optimization without this ramping.

6.5 Optimization settings

There are many settings that need to be specified in order to achieve a good optimization results. These options range from solver options to specific formulations in the actual model. Some of these are general while others need to be chosen manually to fit each specific optimization case. The two main goals when determining these settings have been to get the optimization algorithm to converge within a reasonable amount of time and to get a high result quality, which means a fine discretization and low values on tolerances. The secondary goal is to modify the characteristics of the solution so that it is reasonable and that the right objectives are prioritized.

Solver options

In the Python environment several settings can be manipulated. These affect how the optimization problem is solved. The changes from the default settings that were used in this project are summarized in table 6.2. The tolerances were chosen as low as possible while keeping convergence to a solution. The number of elements affect both the time per iteration and the number of iterations needed to find a solution. For this value a compromise between high resolution and calculation time needs to be made. The blocking factors are used to limit the freedom of the control signal. The notation in the table indicates that the control signals must be constant for each element.

Cost function

The main considerations regarding the cost function is its general formulation and what values the different weights should have. There are two main formulations available, the minimum time formulation and the Lagrange form. In this project only the Lagrange form was considered. Below are the cost functions used in this project for phase 1 (equation 6.1a) and 2 (equation 6.1b).

$$\int_0^{t_f} \alpha_1 \dot{u}^2 + \beta_1 (T_{SH4} - T_{ref,1})^2 + \gamma_1 \dot{u}_p^2 + \delta_1 (p_{SH4} - p_{ref})^2 dt \quad (6.1a)$$

$$\int_0^{t_f} \alpha_2 \dot{u}^2 + \beta_2 (T_{SH4} - T_{ref,2})^2 + \gamma_2 \dot{u}_{ratio}^2 + \delta_2 o_{bypass}^2 dt \quad (6.1b)$$

Here α , β , γ , and δ are different weights, \dot{u} is the gas mass flow input, \dot{u}_p the pressure reference input, \dot{u}_{ratio} the valve opening ratio input, and o_{bypass} the bypass valve opening. It should be noted that all input signal included in the cost functions are being integrated in the model. This kind of formulation makes the optimization algorithm strive for steady state operation of the model with the controlled variables at their desired values and prevents unnecessary control action.

7

Results

7.1 Phase 1

The components assumed to be critical for the first phase, the SH4 header and the separator, proved uncritical during the start-up, as described in the section for case 1 below. The most likely explanation for this result is that other components are more sensitive than the ones considered in this thesis. Therefore a stricter constraint on the SH4 header was introduced in order to illustrate how this phase of the optimization could be conducted. A minimum constraint of -30 MPa was used for the cases 2 and 3. The optimization cases are summarized in table 7.1, while optimization convergence data can be found in table 7.2. The gas mass flow constraint is 0.15 kg/s^2 for all cases. No larger values were tried as this constraint rarely got active. Twelve elements were used in all cases, which created a NLP problem with 10592 equations. For phase 1, with the more restrictive SH4 header stress constraint used, the final live steam conditions are reached in approximately 4000 seconds. One can note that the calculation time for the solver is small compared to the start-up time of the plant, making real time implementations possible.

Case	α	β	γ	δ	Final time / s	Stress reduced	Monotonous gas flow
1	0.0001	0.001	0.0001	0.0001	4000	No	No
2	0.0001	0.001	0.0001	0.0001	8000	Yes	No
3	0.0001	0.001	0.0001	0.0001	8000	Yes	Yes

Table 7.1 The different optimization cases for phase 1. For the cases with reduced stress an SH4 header stress constraint of -30 MPa is used.

Case	Iterations	T_{calc} / s	Solution type
1	51	69.4	Optimal
2	48	61.7	Optimal
3	39	48.6	Optimal

Table 7.2 Optimization convergence data for phase 1. T_{calc} is the calculation time for the solver IPOPT.

Case 1: stress constraint uncritical

Results for the first optimization case considered for phase 1 can be seen in figure 7.1 together with simulation results with the calculated optimal input signals. The gas mass flow and live steam pressure is ramped with maximal speed, with a large overshoot in gas mass flow in order to reach the desired temperature fast. The minimum stress level of -134 MPa for the SH4 header is far from the constraint and corresponds to a stress amplitude of 116 MPa. The corresponding number of cycles, calculated with the Wöhler curve is 15700000. The comparison between the optimization output and the simulation data provides an estimate of how well the optimization algorithm manages to solve the DAE system that represents the optimization model. In general the signals match to a large degree, but some difference can be observed for the SH4 header stress. The separator stress is also uncritical, with the increased temperature only giving a very small dip in stress during the first

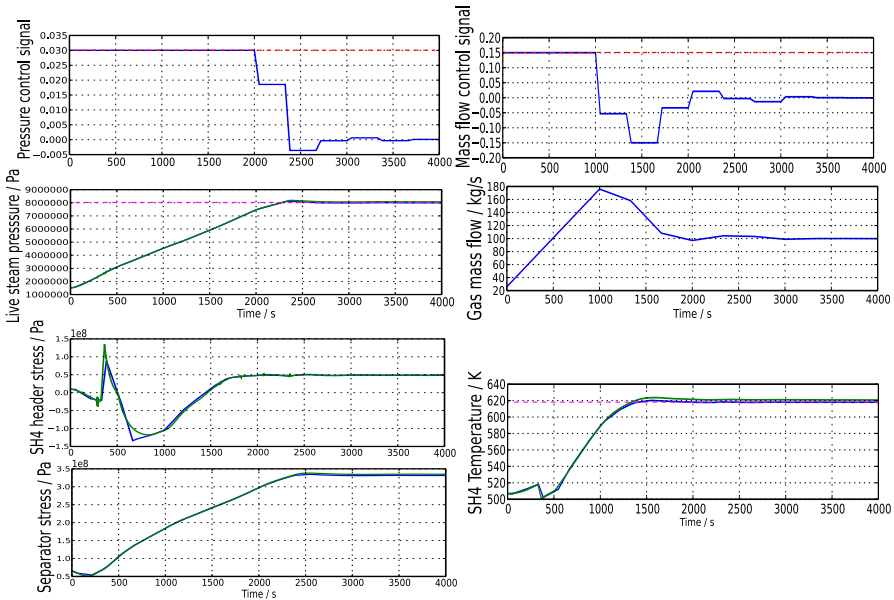


Figure 7.1: The calculated optimal trajectories for phase 1, case 1 in blue together with simulation results with the optimal control signals as input in green. Dashed in red and purple are the active constraints and the setpoints, respectively. One can note that the optimization algorithm manages to represent the system model well, as the difference between the curves is small. The pressure and gas mass flow are ramped at maximal speed. For the gas mass flow a large overshoot compared to the final steady state behaviour can be observed, which makes the temperature reach its setpoint faster.

200 seconds.

Case 2: restrictive SH4 header constraint

Trajectories and optimal control signals for this case, which has a more restrictive SH4 header constraint of -30 MPa, are summarized together with case 3 in figure 7.2. A large overshoot can be observed for the gas mass flow like in case 1. The gas flow is reduced to prevent the constraint from being violated, while the pressure is ramped up at close to maximal speed until the desired value is reached.

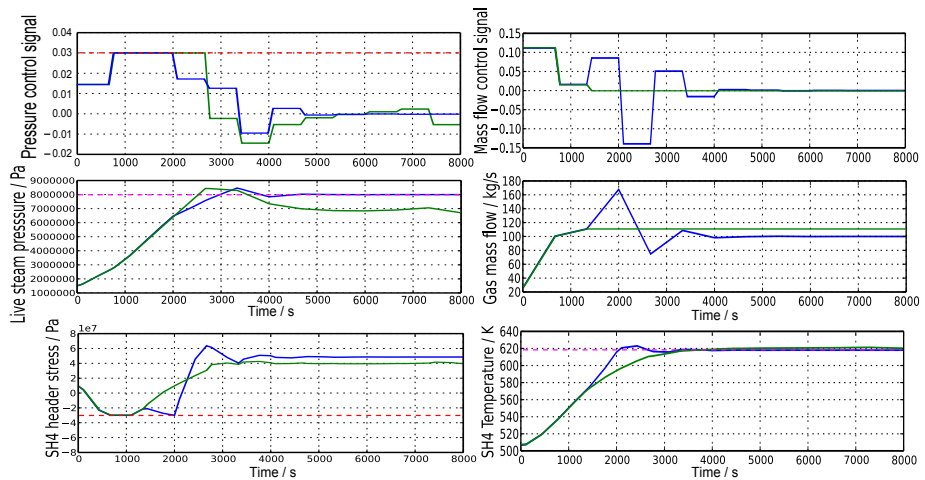


Figure 7.2: The calculated optimal trajectories for phase 1, case 2 in blue and case 3 in green, together with the active constraints marked with dashed red and the desired levels in dashed purple. The active stress constraint forces a reduced increase in gas mass flow compared to case 1. For case 3 only monotonously increasing gas mass flow is allowed. The most notable result for this case is that the live steam pressure does not remain at its desired value for the second half of the optimization time, while the gas mass flow is significantly higher than in case 2. The optimization algorithm prioritizes the faster increase in SH4 temperature the higher mass flow induces over keeping the live steam pressure setpoint. A small deviation from the temperature setpoint can also be observed.

Case 3: monotonously increasing gas mass flow

The results for a case where only monotonously increasing gas mass flow is allowed can be seen in figure 7.2. Interestingly the final conditions of the optimization results are different from the desired working conditions. The live steam pressure is ramped to higher value than the setpoint in order to achieve a faster increase in live

steam temperature. However, it is then decreased to a value of approximately 70 bar, significantly lower than the setpoint of 80 bar. The gas mass flow is ramped to a value around 112 kg/s, which results in too high live steam temperature when the pressure is 80 bar, but gives a more correct temperature for the lower pressure. However the temperature is also slightly too high. The reason for this strange result is that the faster increase in temperature during the first part of the scenario the higher mass flow results in compensates for the constant error in pressure during the last half. However, this result obviously is not practically useful as the desired state for switching to phase 2 is not reached. To avoid this problem additional constraints on pressure and temperature for the final time of the optimization can be implemented.

7.2 Phase 2

The different optimization cases for this phase are summarized in table 7.3. Three different gas mass flow constraints are used, 0.15 kg/s^2 , 0.26 kg/s^2 , and 0.5 kg/s^2 . Depending on the number of elements, 10 for the first four cases and 16 for case 5 and 6, the number of equations in the NLP problems were 100098 and 15792, respectively. Optimization convergence data can be seen in table 7.4. The desired live steam conditions are reached in approximately 3000 seconds with restrictive gas flow changes and 2000 seconds otherwise. The calculated trajectories for the different cases are explained in the following sections.

Case	α	β	γ	δ	Final time / s	Gas flow limit / kg/s^2	Bypass valve reopening
1	0.0006	0.002	14	0.001	7000	0.15	Yes
2	0.00001	0.0005	40	0.001	7000	0.15	Yes
3	0.00001	0.0005	40	0.001	4000	0.26	Yes
4	0.00001	0.0005	40	0.001	4000	0.26	No
5	0.00001	0.0005	40	0.001	4000	0.26	No
6	0.00001	0.0005	40	0.001	4000	0.50	No

Table 7.3 Different cost function weights give different optimization cases. In case 5 and 6 16 elements were used, while 10 elements were used in the rest of the cases.

Case	Iterations	T_{calc} / s	Solution type
1	76	79.7	Optimal
2	56	60.5	Optimal
3	131	167.5	Optimal
4	56	94.0	Optimal
5	57	100.6	Optimal
6	67	118.0	Optimal

Table 7.4 Optimization convergence data for phase 2. T_{calc} is the calculation time for the solver IPOPT.

Case 1: bypass valve reopening

In figure 7.3 optimal control signals are visualized together with the most important model variable trajectories for case 1. The gas flow is increased with maximal control action to reach the desired temperature fast. The stress constraint on the security valve does not get active during this ramping, but the bypass valve is anyway reopened. The most likely reason for this unexpected behaviour is that the weight on the bypass term in the cost function is relatively small, which makes the objective of bypass valve closing less important compared to the SH4 temperature objective. The cost function should still be reduced by closing the valve faster, but it is possible that the difference is smaller than the optimization tolerance.

Case 2: bypass valve prioritized

For this case the weight on bypass valve opening is significantly larger compared to case 1. The effects of this can be observed in the trajectories displayed in figure 7.4. Due to the higher weight the reopening of the bypass valve is smaller in amplitude and the initial closing is more complete. This results in a lower safety valve stress amplitude compared to case 1, as the pressure induced temperature changes are smaller when the valve is operated in a calmer fashion. To investigate if the small reopening of the bypass valve has any indirect affect on the SH4 temperature

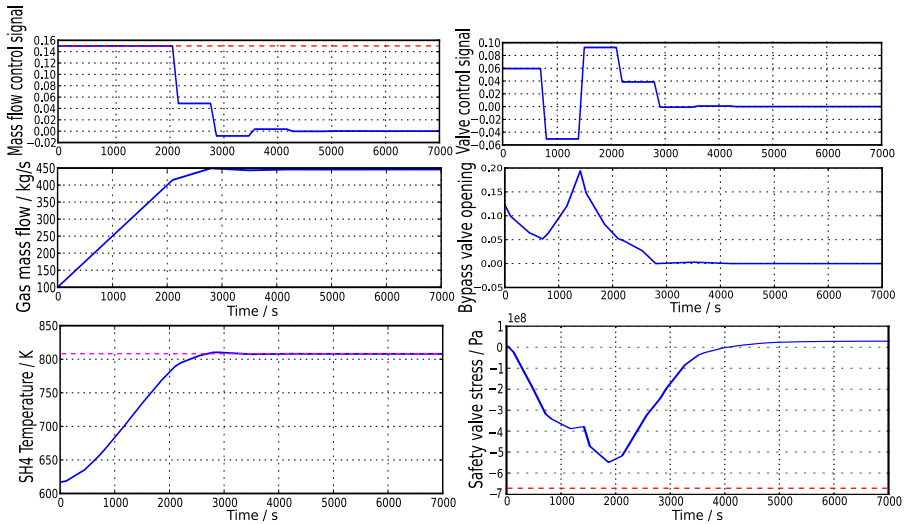


Figure 7.3: The calculated optimal trajectories for phase 2, case 1 in blue, together with constraints marked with dashed red, and the desired SH4 temperature in dashed purple. The gas mass flow is ramped without any overshoot. The stress constraint is not active, yet the bypass valve is reopened.

trajectories from simulations with and without the reopening are also added to the figure. It seems like the reopening has a negligible effect on the temperature.

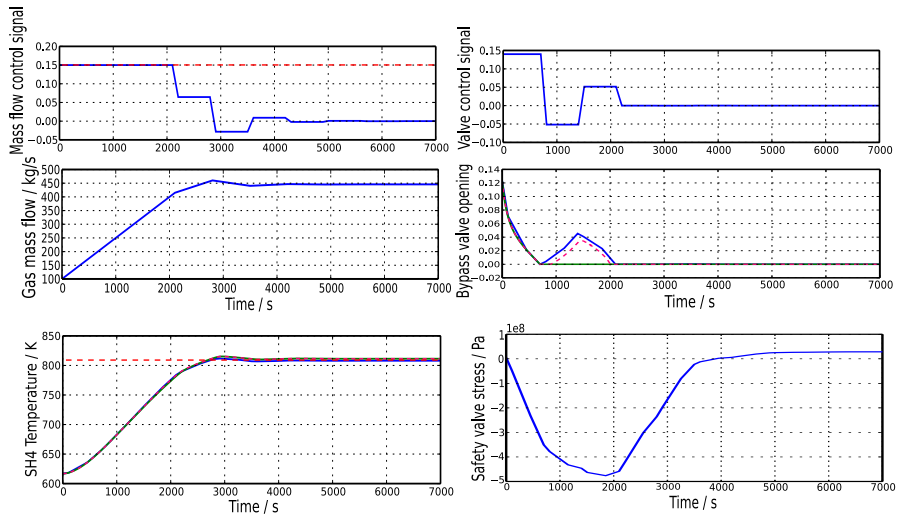


Figure 7.4: The calculated optimal trajectories for phase 2, case 2 in blue, together with simulation results based on the optimization results with (green) and without (pink, dashed) the bypass reopening in the SH4 temperature and bypass valve plots. Constraints are marked in dashed red and the temperature setpoint in dashed purple.

Case 3 and 4: relaxed gas flow constraint

For these cases the gas flow constraint was relaxed. The effect of this can be observed in figure 7.5. Trajectories for both case 3 and case 4 are present in the figure, by this comparison the effect of not allowing redirection of the steam flow through the bypass system can be investigated. The difference is not very big, but the monotonous valve control signal in case 4 forces the gas mass flow signal to become more active in order to prevent the stress constraint from being violated, whereas bypass valve reopening is used for this purpose in case 3.

Case 5: more elements

In this case 16 elements were used rather than 10, which results in a finer discretization. By improving the resolution like this the optimization problem will in general be harder to solve, but the result will be of higher quality. From figure 7.6 one can see a behaviour qualitatively similar to case 4, which has identical settings apart from the discretization. To prevent the stress constraint from being violated the by-

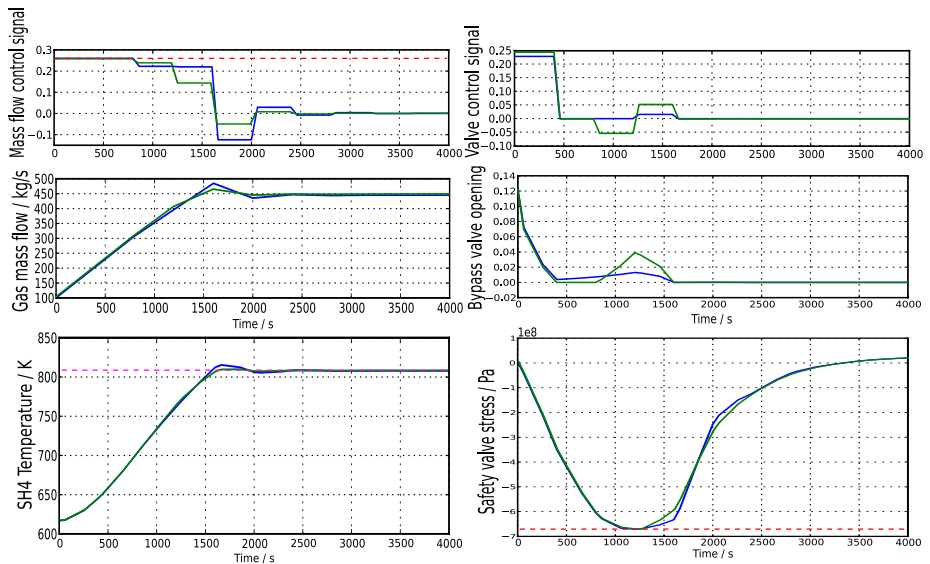


Figure 7.5: A comparison of the calculated optimal trajectories for phase 2, case 3 (blue) and 4 (green). Active constraints are marked in dashed red and the SH4 temperature setpoint is marked in dashed purple. The monotonous valve ratio forces more mass flow control actions in case 4, in order to prevent the stress constraint from being violated.

pass valve is not completely closed and the gas mass flow is slightly decreased after 1000 seconds.

Case 6: extra relaxed gas flow constraints

To investigate how the optimization result is affected by relaxing the gas flow further, the gas mass flow was in this case set to 0.5 kg/s^2 . The settings are otherwise identical to case 5. The results for this case can be seen in figure 7.7, where the trajectories are compared with case 5. It is clear that much more control action is needed to prevent the stress constraint from being violated, when the gas mass flow constraint is less limiting. In this case the optimizer manages to find a solution that keeps the stress close to its limit for approximately 600 seconds. As in previous cases with no bypass valve reopening reducing the gas mass flow is the main tool for preventing constraint violation.

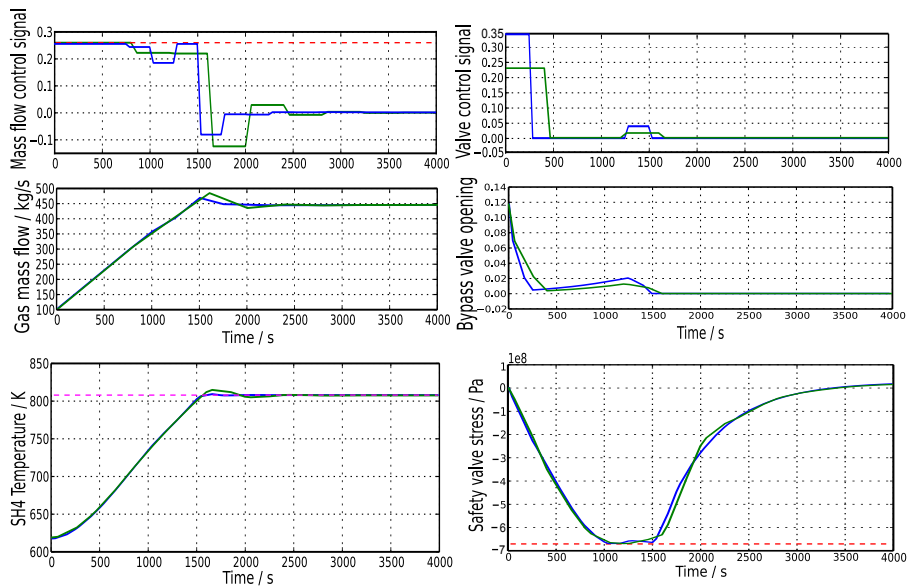


Figure 7.6: The calculated optimal trajectories for phase 2, case 4 in green and case 5 in blue, together with constraints marked with dashed red and the desired SH4 temperature in dashed purple. The control action is similar for the two cases.

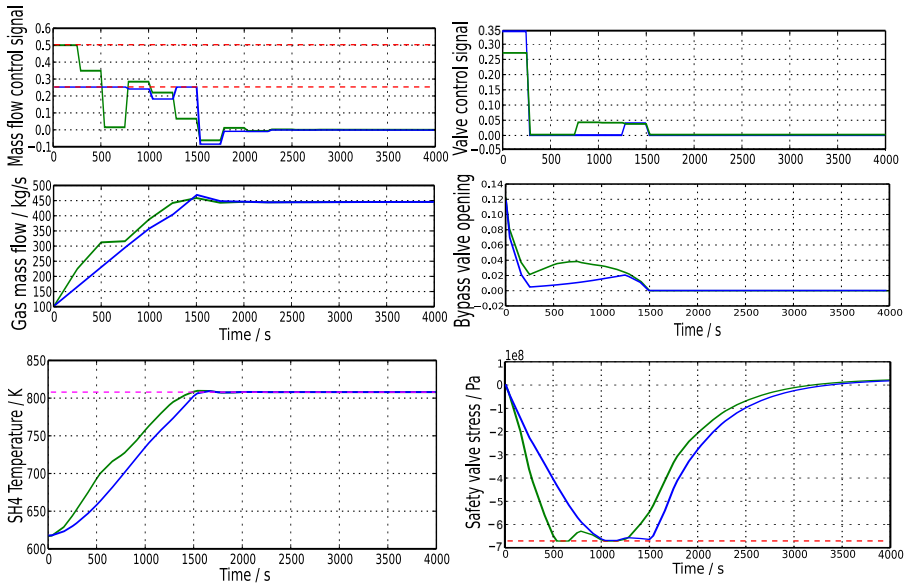


Figure 7.7: The calculated optimal trajectories for phase 2, case 5 in blue and case 6 in green, together with constraints marked with dashed red and the desired SH4 temperature in dashed purple. In case 6 the further relaxed gas mass flow constraint results in a slightly longer period with stress close to the limit compared to case 5.

8

Discussion and Conclusions

8.1 Modelling

The level of complexity of the optimization model is believed to capture most of the relevant behaviour of the real plant. However, as the number of matching parameters in the model is quite large, the parameter values chosen in this project are not the optimal ones and therefore a clear difference can be observed for some variables, especially many of the gas temperatures. One could also argue that the cause for this is that not all of the heat exchangers in the real plant have exact counterparts in the optimization model, since the heat exchangers in the model in some cases represent not only the corresponding heat exchanger in the real plant, but also some heat exchange happening in between the heat exchangers.

Furthermore, the matching between the models is only verified for close to full load. In order to get a more useful optimization model it is necessary to make sure that the behaviour of the model is also correct for lower loads.

Further work

There are two main directions for improving the optimization model so that the behaviour gets more similar to the real plant. The first is to improve parameter values, such as heat transfer coefficients, boundary conditions and control system parameters and setpoints. It would be desirable to decide these values in a systematic manner with the objective of matching the real plant in the range of temperatures, pressures and mass flows that are present during the start-up. Grey-box identification could be a suitable technique for this purpose.

The second direction is to improve the components and structure of the plant model to improve its behaviour. There are many phenomena not accounted for in the current model such as heat transfer through radiation, heat transfer in between heat exchangers, and the spray water cooling system. However, whenever new physical phenomena are added to the model, it is important to verify that the increase in

accuracy is large enough to compensate for the extra complexity in the optimization. For this reason another possible step in the modelling task would be to reduce the number of heat exchangers to investigate if the dynamics between input and output for the whole chain of heat exchangers could be described by a simpler system. If the decrease in accuracy would not be too great this could be a way to simplify the system, which would make the optimization problem less complex. However, having a model structure similar to the real plant has clear benefits apart from giving better accuracy, as it simplifies the choice of parameter values and improves the general understandability of the model.

To develop a coal and flue gas media model suitable for optimization could also increase the accuracy of the model. This would bring the extra benefit of removing at least some of the empiric parameters in the heat exchangers, as heat capacities and possibly other medium properties could be calculated automatically instead. Whether it is worthwhile to introduce a mill and combustion system is an interesting question. In the current model the change in gas mass flow is assumed to be directly controllable, something that is not true for the real plant. The question is if the proposed optimal mass flow schedule can be achieved by the corresponding system in the real plant. If this is the case it would be unnecessary to add these components as they have no other affect on the model. If it is not possible to achieve this mass flow one would need to consider adding extra components, or at least alter the constraints on the gas mass flow to fit the behaviour of the real plant.

8.2 Optimization

Compared to the previous project regarding the Jänschwalde plant, great improvements have been achieved regarding the optimization despite a significantly greater model complexity. However, more work is needed before the control algorithms developed in this thesis could be applied to the real plant.

In this project variable scaling and state selection have both proven important for achieving good optimization results. Improvements in these areas are the biggest reason for the improved result quality. It is however still worth investigating the state selection further, as density might not be optimal for components where only liquid water is present.

By comparing different optimization cases it is clear that the optimal trajectories are highly dependent on optimization settings such as cost function weights. This is desirable in the sense that it gives freedom to the user to manipulate the behaviour of the plant during the start-up scenario, but it also means that more work is needed to decide which objectives that should be prioritized. If more constraints are introduced into the model to account for the limitations of the real plant this phenomenon would probably be reduced.

Possible improvements

As there are many parameters to determine for the optimization problem, the setup chosen in this project is not the optimal. The general strategy when deciding these parameter values has been to attempt to find good values for each parameter independently. Due to the number of settings possible this is the only method one could use within a reasonable time frame and by spending time finding better values for these parameters better discretization and tolerance levels could probably be achieved.

A step that might result in a more optimal result would be to handle both the phases in the start-up as one optimization problem. The current setup, with a fixed point in which the optimization inputs and objectives are changed might not give an optimal result. Firstly, the second part of the optimization is not considered during phase one. Secondly, there might be a better switching point. However, one needs to be careful when deciding whether to change this, as it might get harder to implement the control in the real plant if the calculated start-up schedule is too different from the current scheme.

To get better optimization results one could also try using the optimization software on a system with more computational power. This would increase the speed of the optimization, which would make it possible to run optimizations with more iterations or with more calculations (meaning finer discretization or more complex model) per iteration. However, during this project the computational time can not be said to have been a too limiting factor.

The optimization problem formulation could also be improved. The objective of the optimization would be better defined by including terms such as generated power or fuel consumption in the cost function. By doing this the environment and financial gains from optimizing the start-up procedure would be clearer and the choice of cost function weights would become less arbitrary. A minimum time formulation could also be evaluated, something that has not been tried during this thesis.

8.3 Experiences with JModelica.org

The JModelica.org platform has proven very powerful for optimization purposes during this thesis. Solutions to all reasonable optimization problem formulations tried in the project have eventually been found and in general the optimization software has not been a limiting factor. However, some aspects of the platform could be improved. Currently much time needs to be spent on issues such as scaling and in many cases the convergence of the optimization algorithm is very sensitive to parameter changes and the working conditions of the model.

If some of this work could be handled automatically by the tool and if the interaction with the program could be simplified for the user it would be less time consuming to investigate different optimization cases. Some suggested improvements

are therefore a better handling of variable scaling and equation scaling. To introduce shifting of variables could also be considered, as well as a general improvement of the user interaction, possibly with a graphical interface. Some of these issues might however be resolved with the introduction of the CasADi platform.

The following specific problems with the software were encountered throughout the course of the project:

- Poorly scaled equations caused problems, when trying to simulate FMU models with JModelica.org for certain versions of the platform.
- Certain formulations of initial equations made it impossible to simulate FMU models.

8.4 Conclusion

The results of this thesis show that it is possible to develop reasonably complex optimization cases for thermal power plant start-ups using JModelica.org and Dymola. However, to achieve this, one needs to focus on adapting every part of the model so that it is suitable for optimization. As JModelica.org is a platform under development some aspects of this process might be simplified in the future.

During the project it has also been observed that the matching of a simplified model to a more complex one is a difficult task to perform by hand for models of this complexity. Changing one parameter value typically affects the model in more than one way, which makes it hard to decide correct values as the parameters can not be treated independently.

A big remaining step between the function of the current optimization model and the usage of it in the real plant is the matching of the two systems. Despite the similarities between the two systems there are also large differences, both in terms of the physical modelling and the control systems. In order to implement control strategies developed with JModelica.org more work is needed. The optimization model needs to be developed further and some alterations of the control of the real plant are probably also needed. A suitable next step towards this goal would be to use an optimization model to calculate the control signals during a simulation of a start-up scenario of the detailed plant model. By doing this one would get a very good indication of how an implementation for the real plant would work. Another possible approach would be to use optimal trajectories calculated with JModelica.org to develop the start-up strategy off line. This method would be simpler as it does not require any direct interaction between the systems.

Bibliography

- Åkesson, J., K.-E. Årzén, M. Gäfvert, T. Bergdahl, and H. Tummescheit (2010). “Modeling and optimization with Optimica and JModelica.org—languages and tools for solving large-scale dynamic optimization problems”. *Computers and Chemical Engineering* **34**:11, pp. 1737–1749.
- Alvarez, H. (2006a). *Energiteknik del 1*. Studentlitteratur, Lund.
- Alvarez, H. (2006b). *Energiteknik del 2*. Studentlitteratur, Lund.
- Andersson, C., J. Åkesson, C. Führer, and M. Gäfvert (2011). “Import and export of functional mock-up units in jmodelica.org”. In: *8th International Modelica Conference*. Dresden, Germany.
- Andersson, E. (2013). *Development of a dynamical model for start-up optimization of coal-fired power plants*. MA thesis. KTH. URL: <http://www.control.lth.se/documents/1999/5629.pdf>.
- Bauer, O. (1999). *Modelling of two-phase flows with Modelica*. MA thesis. Department of Automatic Control, Lund University, Sweden. URL: <http://www.control.lth.se/documents/1999/5629.pdf>.
- Biegler, L. T., A. M. Cervantes, and A. Wächter (2001). “Advances in simultaneous strategies for dynamic process”. *Chemical Engineering Science* **57**, pp. 575–593.
- Casella, F, M Farina, F Righetti, R Scattolini, D Faille, F Davelaar, A Tica, H Gueguen, and D Dumur (2011). “An optimization procedure of the start-up of combined cycle power plants”. In: *18th IFAC world congress*. Milano, Italy, pp. 7043–7048.
- Dietl, K, S Gallardo Yances, A Johnsson, J Åkesson, K Link, and S Velut (2014). “Industrial application of optimization with modelica and optimica using intelligent python scripting”. In: *10th International Modelica Conference*. Lund. *FMI*. <https://www.fmi-standard.org/>. Accessed 2014-05-06.

- Hübel, M, A Berndt, S Meinke, M Richter, P Mutschler, E Hassel, H Weber, M Sander, and J Funkquist (2014). “Modelling a lignite power plant in modelica to evaluate the effects of dynamic operation and offering grid services”. In: *10th International Modelica Conference*. Lund.
- IPOPT*. <https://projects.coin-or.org/Ipopt>. Accessed 2014-05-06.
- JModelica.org User's guide* (2014). <http://www.jmodelica.org/page/6212>. Accessed 2014-05-10.
- Kraftwerk Jämschalde* (2012). Plant handbook, internal document. Vattenfall.
- Lind, A. and E. Sällberg (2012). *Optimization of the Start-up Procedure of a Combined Cycle Power Plant*. MA thesis. Department of Automatic Control, Lund University, Sweden.
- Ljung, L. and T. Glad (2004). *Modellbygge och simulering*. Studentlitteratur, Lund.
- Meinke, S. (2012). *Modellierung thermischer Kraftwerke vor dem Hintergrund steigender Dynamikanforderungen aufgrund zunehmender Windenergie- und Photovoltaikeinspeisung*. PhD thesis. Rostock University.
- MODRIO*. <https://itea3.org/project/modrio.html>. Accessed 2014-04-28.
- Palmkvist, E. (2014). *Implementation of grey-box identification in JModelica.org*. MA thesis. Department of Automatic Control, Lund University, Sweden. URL: <http://www.control.lth.se/documents/2014/5941.pdf>.
- Saarinen, L., K. Boman, and J. Funkquist (2011). “Dynamic model of a boiler at the jämschalde plant”. Vattenfall Research and Development AB. Älvkarleby.
- Sundén, B. (2006). *Värmeöverföring*. Studentlitteratur, Lund.
- Vattenfall*. <http://powerplants.vattenfall.com/node/288>. Accessed 2014-03-06.
- Wächter, A. (2009). *Short Tutorial: Getting Started With Ipopt in 90 Minutes*. IBM T.J. Watson Research Center, New York, USA. URL: <http://drops.dagstuhl.de/volltexte/2009/2089/pdf/09061.WaechterAndreas.Paper.2089.pdf>.

Lund University Department of Automatic Control Box 118 SE-221 00 Lund Sweden		<i>Document name</i> MASTER 'S THESIS	
		<i>Date of issue</i> August 2014	
		<i>Document Number</i> ISRN LUTFD2/TFRT--5950--SE	
<i>Author(s)</i> Håkan Runvik		<i>Supervisor</i> Stéphane Velut, Modelon AB Anders Robertsson, Dept. of Automatic Control, Lund University, Sweden (examiner)	
		<i>Sponsoring organization</i>	
<i>Title and subtitle</i> Modelling and start-up optimization of a coal-fired power plant			
<i>Abstract</i> <p>In the German electrical market, where almost no hydro power is present, the demand for regulating power is rising. The main reason for this is the expansion of solar and wind power, which is desirable from an environmental standpoint, but also introduces large and fast variations in production. To keep the necessary balance between production and consumption, the operation of thermal power plants is changing, both in terms of stand still time and load variations. For this reason the start-up procedure of the Vattenfall owned German lignite power plant Jämschalde is investigated in this thesis.</p> <p>A model is created that is complex enough to describe the behaviour of the real plant reasonably accurately, while at the same time simple enough so that optimization of it can be performed with the optimization platform JModelica.org. A detailed plant developed in another thesis is used to determine parameter values and validate the behaviour of the optimization model during simulation. The startup procedure is handled as an optimal control problem, with constraints on stress in order to avoid damage and maximize the life length of components. Results for different optimization cases are finally calculated and compared.</p>			
<i>Keywords</i> JModelica.org, Dynamic optimization, Modelica, Control, Modelling, Thermal power plants			
<i>Classification system and/or index terms (if any)</i>			
<i>Supplementary bibliographical information</i>			
<i>ISSN and key title</i> 0280-5316			<i>ISBN</i>
<i>Language</i> English	<i>Number of pages</i> 1-61	<i>Recipient's notes</i>	
<i>Security classification</i>			